Measuring Dielectrics Using Shielded Loop Antennas

by

Nathan Yiin

A Thesis Presented in Partial Fulfillment
of the Requirements for the Degree
Master of Science

Approved April 2018 by the
Graduate Supervisory Committee:

James Aberle, Chair
Bertan Bakkaloglu
Jennifer Kitchen

ARIZONA STATE UNIVERSITY

May 2018

ABSTRACT

This work is concerned with the use of shielded loop antennas to measure permittivity as a low-cost alternative to expensive probe-based systems for biological tissues and surrogates. Beginning with the development of a model for simulation, the shielded loop was characterized. Following the simulations, the shielded loop was tested in free space and while holding a cup of water. The results were then compared. Because the physical measurements and the simulation results did not line up, simulation results were forgone. The shielded loop antenna was then used to measure a set of NaCl saline solutions with varying molarities. This measurement was used as a calibration set, and the results were analyzed. By taking the peak magnitude of the input impedance of each solution, a trend was created for the molarities. Following this measurement and analysis, a set of unknown solutions was tested. Based on the measurements and the empirical trends from the calibration set of measurements, the molarities of the valid unknown solutions were estimated. It is shown that using the known molarities, permittivity can also be calculated. Using the estimated molarities of the unknown solutions, the permittivity of each solution was calculated. The maximum error for the estimation was 1.07% from the actual data.

DEDICATION

To my family, my friends, and everyone who believed in me

TABLE OF CONTENTS

Page

LIST OF TABLES

LIST OF FIGURES

Figure Page

Figure Page

Figure Page

Figure Page

CHAPTER 1

INTRODUCTION

Determining the dielectric properties of materials is useful for understanding the nature of the material as well as the interaction between electro-magnetic fields within the material. A number of methods for measuring and monitoring the dielectric properties exist, and among these are methods of using pulse delay oscillators or measuring reflection and transmissions through a sample of material [1].

However, when considering biological tissues and commercially available surrogates for such tissues, many of these methods are not feasible, because biological substances are liquid or semi-liquid substances with complex permittivity. Specialized high frequency probes for measuring the permittivity of biological materials were first developed around 1980, as demonstrated with an open-ended coaxial line as a sensor for *in vivo* and *in vitro* [2]. In measurements with synthetic materials or in tissues, it becomes necessary to monitor the relative permittivity of the material, to ensure that as testing continues, the material does not degrade beyond the point of practical use.

The major contribution of this thesis is to investigate the feasibility of using simple, low-cost measurements and simulations to monitor the permittivity, and hence the quality, of commercially available tissue surrogates. This approach contrasts with expensive probe-based systems that have been used to monitor material quality, or worse, not being able to determine if the material has degraded, possibly invalidating any results that have been obtained.

A shielded loop antenna is well suited for measuring liquid or semi-liquid substances because it has a broadband response by virtue of a uniform resistive loading,

which reduces magnetic response while leaving the electrical response relatively unaffected [3]. This thesis will discuss measuring the permittivity of various materials using shielded loop antennas and applied radio frequency (RF) energy.

This thesis begins with literature review on loop antennas and measuring dielectrics. In chapter 2, the design method is discussed in length, including the simulation results. Chapter 3 details the experimental results, and chapter 4 shows the detailed analyses for the results. Finally, chapter 5 summarizes and concludes the project and includes a brief acknowledgement section.

CHAPTER 2

LOOP ANTENNAS AND MEASURING DIELECTRICS

Loop antennas can take many different forms, but the circular loop is by far the most popular, because of its relative simplicity in terms of both analysis and construction. A small loop antenna "is equivalent to an infinitesimal magnetic dipole whose axis is perpendicular to the plane of the loop" [4]. Circular loops are classified based on their overall length, that is their circumference, as electrically small ($C < \lambda/10$) or electrically large ($C \sim \lambda$) and have varied applications from 3MHz to 3GHz, and field probe applications in the microwave frequency range [4].

The input impedance of a loop antenna in transmitting mode can be modelled using the equivalent circuit show in Figure 2.1.

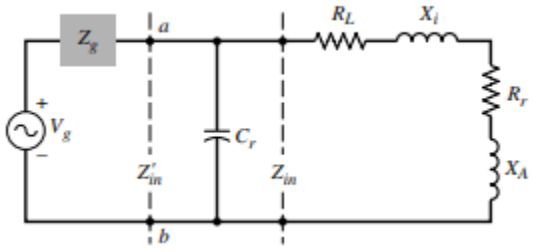

Figure 2.1 Equivalent Circuit of a Transmitting Mode Loop Antenna [4]

Loop antennas are inefficient radiators, and thus are not used much for transmission, but are more commonly used in receiving mode, specifically for radios and pagers (radio communication) and as probes for field measurements. Electrically large loop antennas have also been used as directional antennas for navigation [4]. Shielded loops have also been demonstrated for having applications in wireless power transfer in near field (inductive coupling), as both transmitters and receivers [5].

The three major applications of non-free-space conditions of shielded loop antennas are “seawater communications, ground sensing / communications, and human body sensing / communications” [5]. These mediums affect both the propagation and the impedance of the antenna [5].

As aforementioned, dielectric measurements have been demonstrated using a variety of methods, including pulse delay oscillators (which measure altered phase velocities along a shortened transmission lines), pairs of antennas in broadband transmitting and receiving modes (which measure using frequency-domain methods), and resonators (which measure the resonant frequency and thickness and use a sample material with known values as a relation) [1]. These methods are suitable for simple permittivity measurements. Complex permittivity measurements require other methods, such as open-ended coax cables and short monopole antennas. Short monopole antennas have been demonstrated for measuring dielectrics both *in situ* and *in vivo* [6]. These methods require computer-controlled network analyzers to process the data to gain accurate readings and measurements [2].

The shielded loop discussed here is different than these previous works for several reasons. Resonators, pulse delated oscillators, and pairs of antennas are useful for measuring dielectrics in narrow bandwidths, but shielded loop antennas are useful for broad bandwidth applications. Since complex permittivity measurements rely on computer network analyzers to measure the input impedance, this method of measurement is retained. However, the setup in this experiment is mainly through an RF detector and probe, and measuring the input impedance of a known dielectric material.

This initial measurement is a calibration measurement, and subsequent measurements will indicate direct changes in the input impedance.

CHAPTER 3

DESIGN METHOD

Based on previous research at ASU, a shielded loop antenna provided by Dr. Diaz and his PhD students was used for initial research purposes. This shielded loop was fabricated using RG-141A transmission line, and a photograph of the device is shown in Figure 2.1. The overall outer shielding of the coaxial cable was covered with tin solder which also connected the two pieces.

Figure 3.1 Shielded Loop Antenna Used for Initial Simulations

Since no mechanical drawing or electromagnetic simulation files existed, the dimensions of the shielded loop antenna needed to be measured, a mechanical model developed, and then simulated in Ansys HFSS. An example of the shielded loop model captured from HFSS can be seen in Figures 3.2 and 3.3.

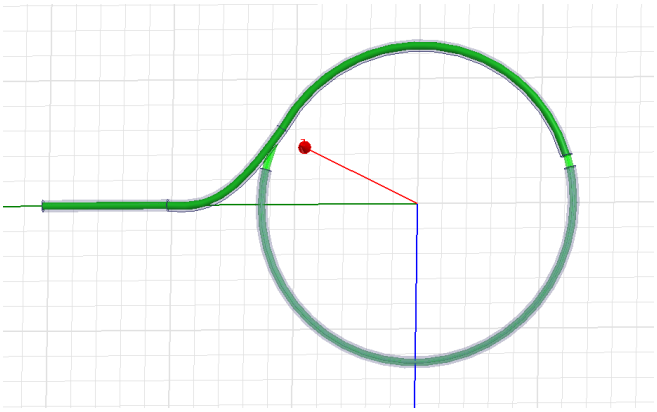

Figure 3.2 Top view of the shielded loop antenna in HFSS

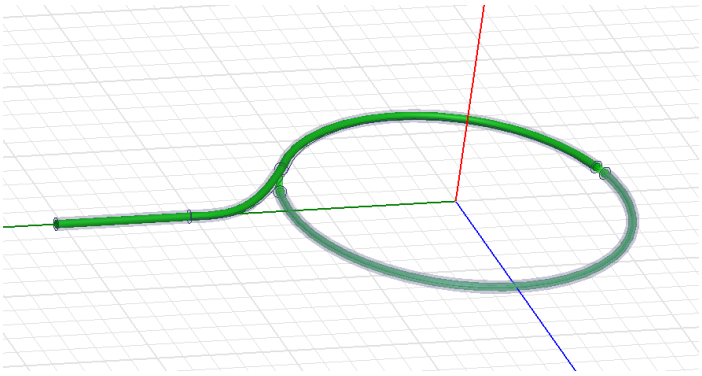

Figure 3.3 Plan view of the shielded loop antenna in HFSS

Certain assumptions were made when building this shielded loop antenna in simulation. Tin was assumed to not change the overall wave propagation, and thus tin cylinder structures to cover the waveguide were used rather than a sheet of tin and a small arc of tin was used to connect the two pieces on the far side. In Figure 3.2, the top side of the shielded loop is not perfectly circular, as it needed to be joined together with the input of this coax.

Using the solution frequency of 915MHz, the characteristic impedance of the waveport at the input of the coaxial feedline was obtained using HFSS, and the result can be seen in Figure 3.4. The value obtained is reasonably close to the nominal value of 50Ω for RG-141A coaxial cable.

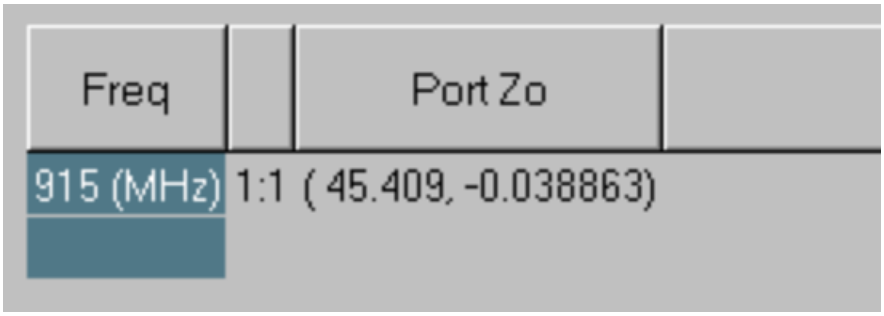

Figure 3.4 Characteristic impedance of the shielded loop antenna

The characterization of this antenna requires the input reflection coefficient S(1,1) and the input impedance, found using the Z(1,1), as this is a one-port. The magnitude of S(1,1) in dB and the magnitude of Z(1,1) obtained using HFSS for the shielded loop placed in an otherwise empty universe are seen below in Figure 3.5 and Figures 3.6.

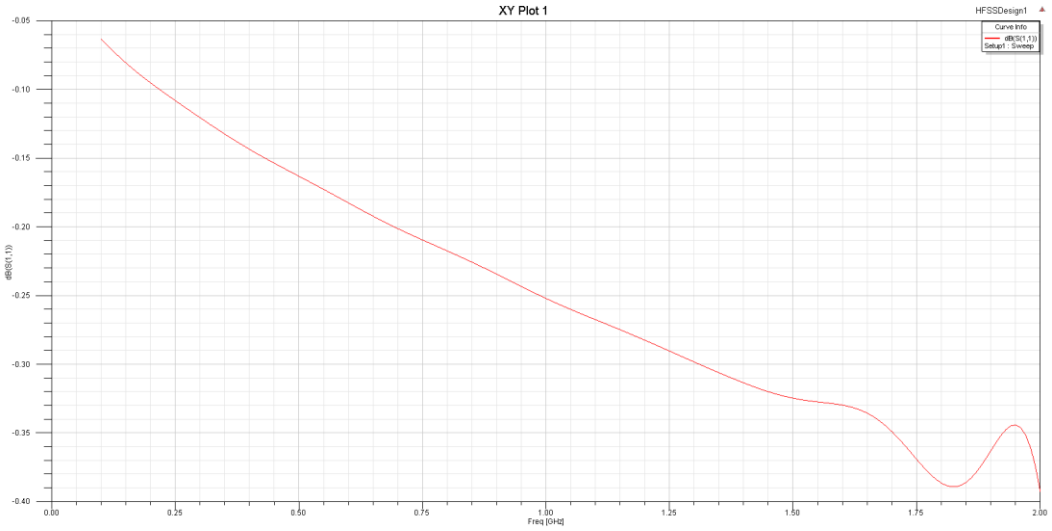

Figure 3.5 S(1,1) in dB during a frequency sweep from 0.1 to 2 GHz

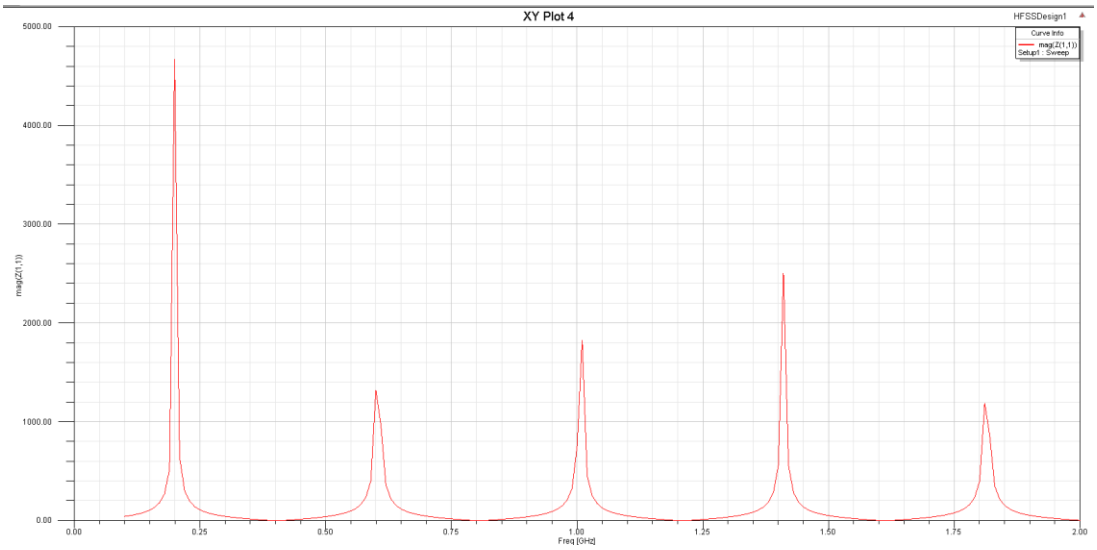

Figure 3.6 Z(1,1) in magnitude during a frequency sweep from 0.1 to 2 GHz

After this simulation was completed, a structure was also modelled to simulate approximately the experimental apparatus. This structure includes a cylinder of distilled water inside the shielded loop and can be seen in Figures 3.7 and 3.8.

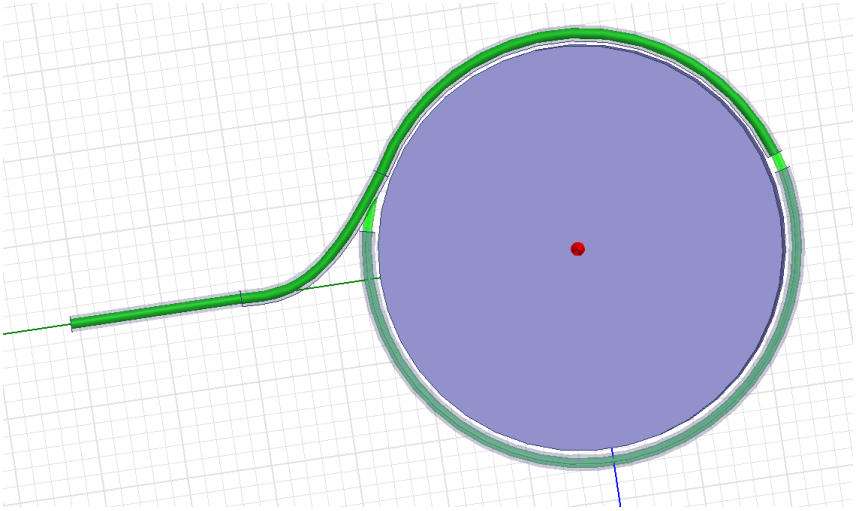

Figure 3.7 Top view of the approximate geometry of the experimental apparatus

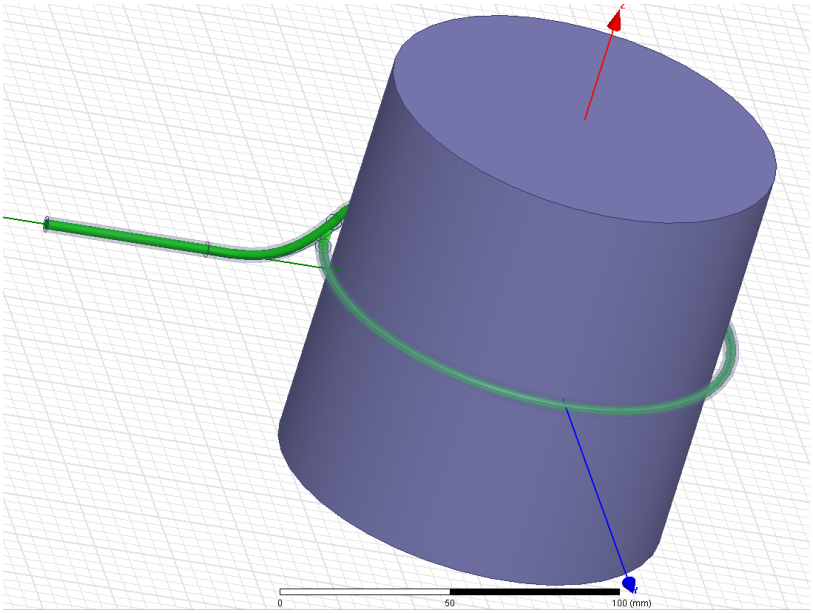

Figure 3.8 Plan view of the approximate geometry for the experimental apparatus

Several assumptions were also made when simulating this apparatus. The shielded loop was assumed to be positioned perfectly in the middle of the cylindrical structure of water. It was assumed that the plastic cup holding the water would have a negligible effect on the overall input impedance when measuring the dielectric, so no plastic cup structure was created. As aforementioned, the shielded loop is also not perfectly circular, and thus, there is a change in spacing between the sides of the antenna, which was assumed to have negligible effect on the overall effect on the input impedance.

This structure was simulated with the solution frequency of 915MHz. The resulting characteristic impedance is seen in Figure 3.9.

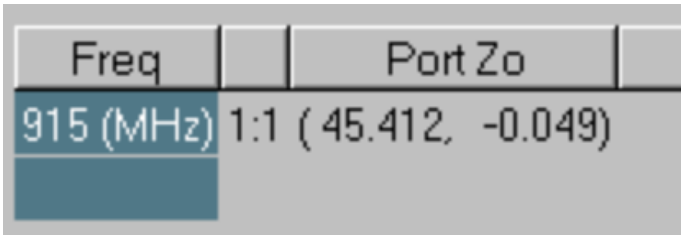

Figure 3.9 Input impedance of the approximate geometry of the experimental apparatus

The characteristic impedance is affected negligibly by including the water and is still close to the ideal 50Ω impedance. This result makes sense since the fields within a coaxial cable transmission line reside entirely between the inner and outer conductors, and are not affected by the external environments.

As for the situation of the shielded loop antenna in free space, a frequency sweep was performed to verify that the models were in fact working properly. The frequency sweep checked for the reflected power S(1,1) and the magnitude of Z(1,1) are shown below in Figures 3.10 and 3.11.

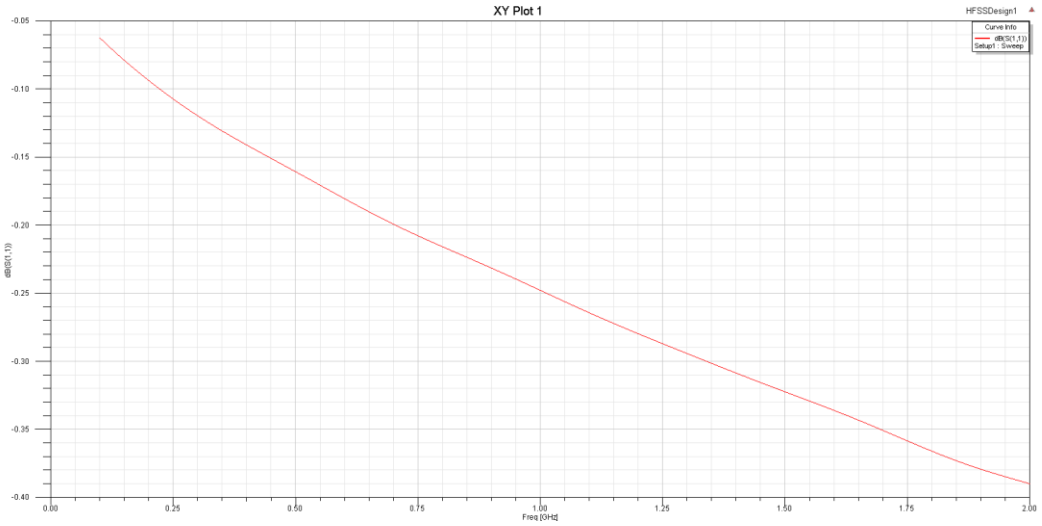

Figure 3.10 S(1,1) in dB during a frequency sweep from 0.1 to 2 GHz for the experimental apparatus

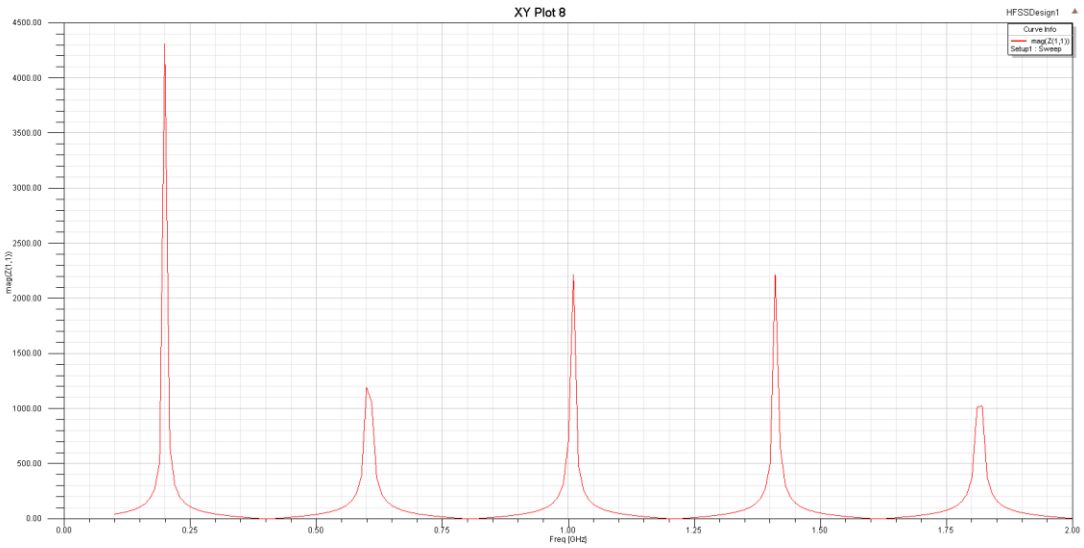

Figure 3.11 Z(1,1) in magnitude during a frequency sweep from 0.1 to 2 GHz for the experimental apparatus

CHAPTER 4

DATA ANALYSIS AND DISCUSSION

Comparison of Simulation and Measurements Results

The first set of experiments were performed in the instructional lab (GWC 326) using the FieldFox VNA. The purpose of these experiments was to qualitatively validate the results from the HFSS simulations. In the first of these experiments, the impedance of the shielded loop by itself was measured. This experimental setup can be seen in Figure 4.1.

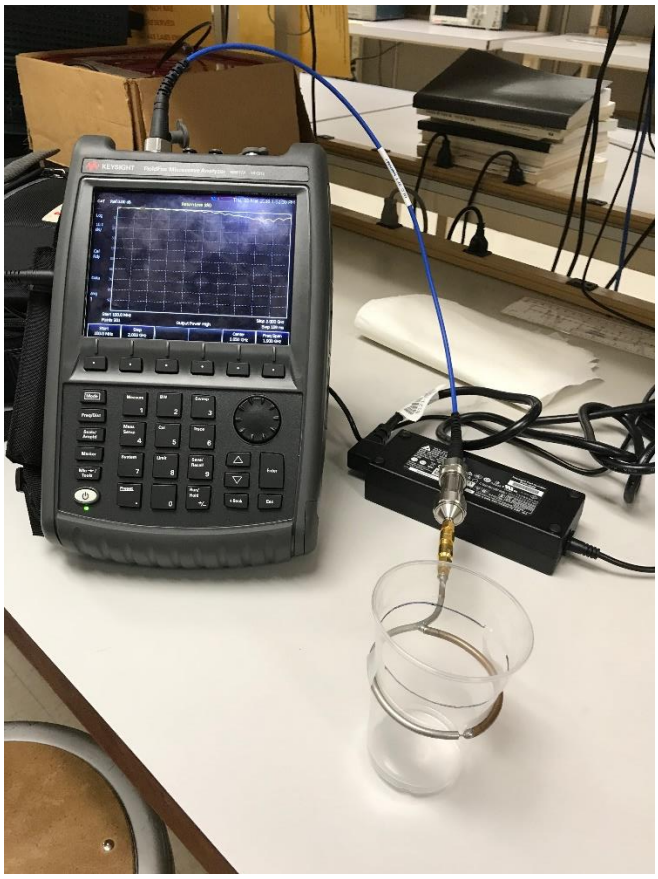

Figure 4.1 Initial experimental setup for measuring the impedance of the shielded loop antenna with the FieldFox

Using the VNA, the data was saved as a Touchstone *.s1p file and imported into ADS for further analysis. The reflection coefficient S(1,1) in dB, and the magnitude of Z(1,1) are seen below in Figures 4.2 and 4.3.

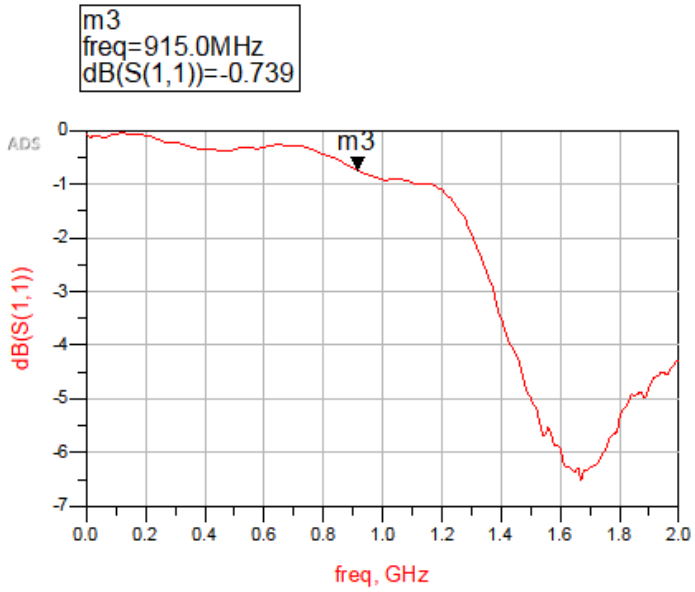

Figure 4.2 Reflected power in free space

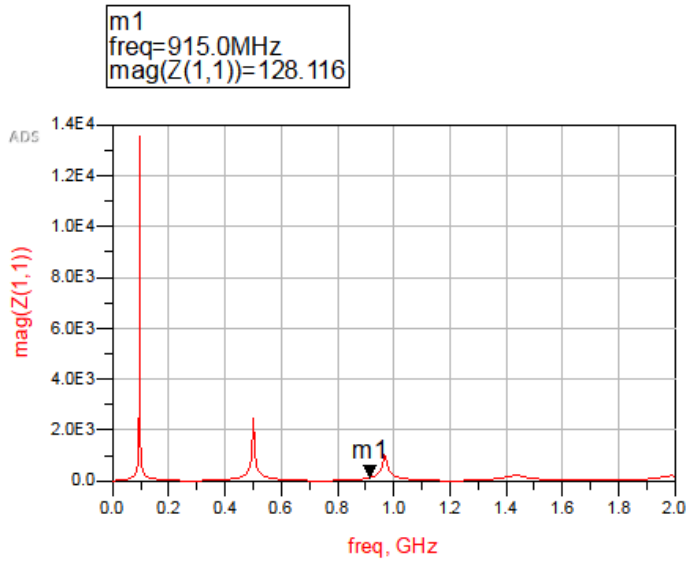

Figure 4.3 Input impedance across frequencies

The input impedance was separated into real and imaginary portions, as seen in Figure 4.4.

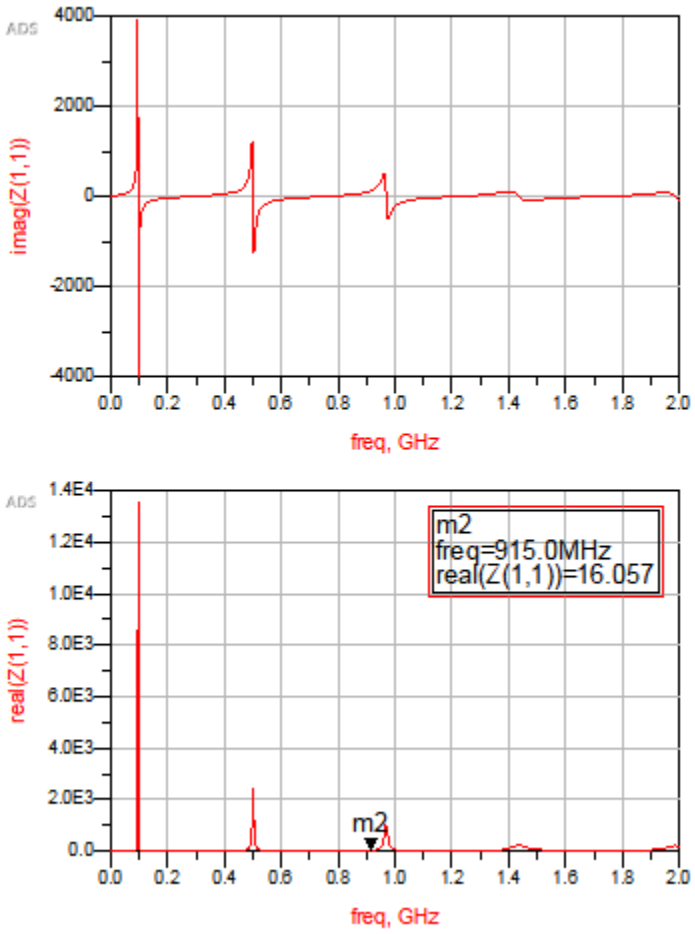

Figure 4.4 Imaginary (top) and real (bottom) of the input impedance in free space

The next experiment was to see the base impedance profile of water, which has a high relative dielectric (80). This setup can be seen in Figure 4.5.

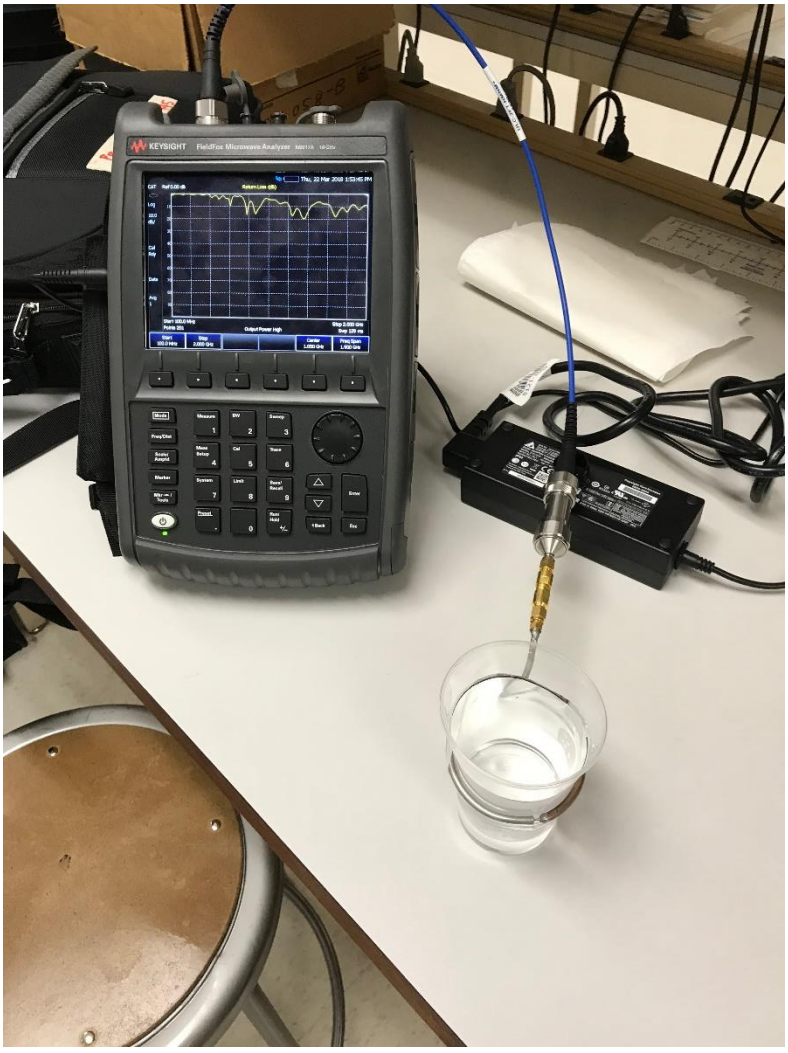

Figure 4.5 Initial experimental setup with water

The VNA was used to obtain the data for this experiment, and that data was then analyzed in ADS. The reflection coefficient in dB is seen below in Figure 4.6, and the magnitude of the input impedance is shown in Figure 4.7.

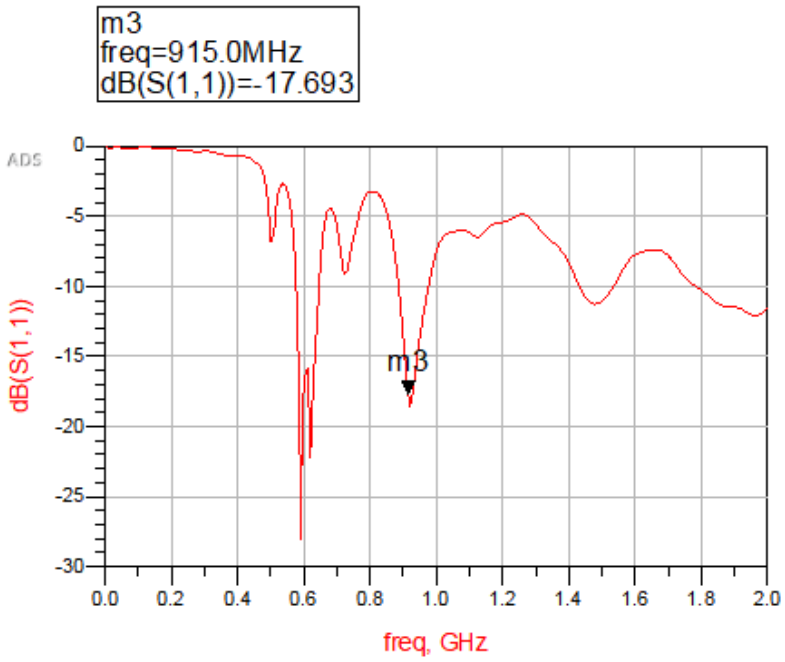

Figure 4.6 Reflected power with a cup of water

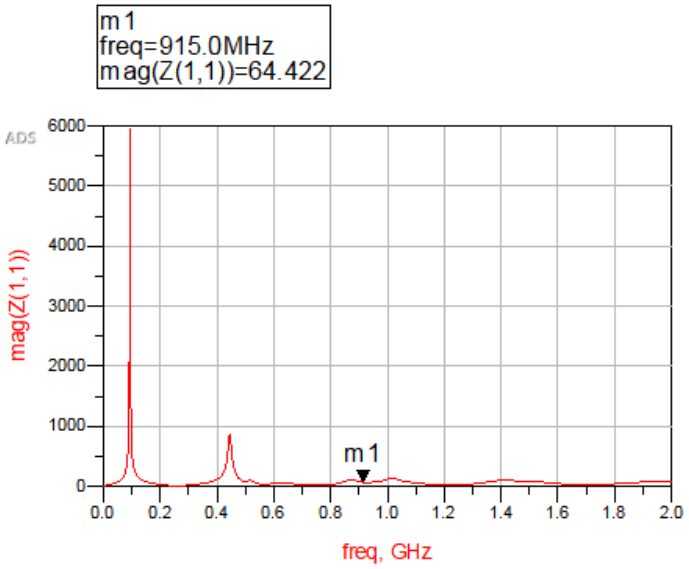

Figure 4.7 Input impedance with a cup of water

The real and imaginary parts of the input impedance are shown below in Figure 4.8.

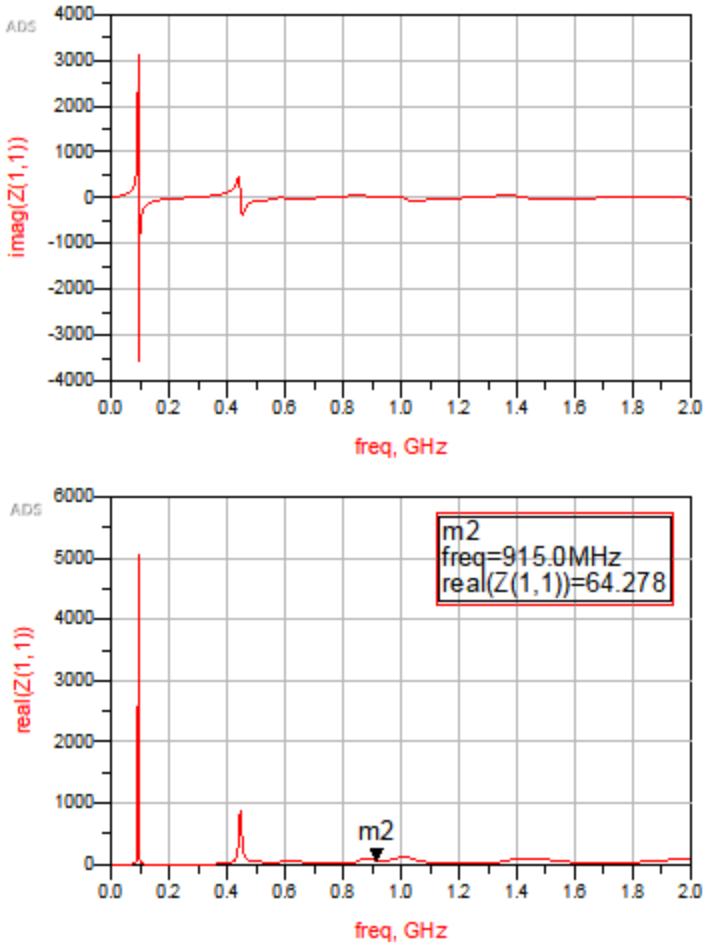

Figure 4.8 Real and imaginary parts of Z(1,1)

This setup was originally chosen because of its overall similarity to how a tissue surrogate sample would be measured—a portable VNA in a general lab space with other equipment necessary for other biological measurements. A portable VNA would also allow for consistent monitoring of multiple experimental setups. However, it is evident that there was a great deal of noise in the measurement because of all the various objects and people within the area (referring to the free space measurement), so it was decided to repeat the measurements in the electromagnetic anechoic chamber facility in ECG to reduce the noise within the measurements and obtain more accurate results. The setup in the facility can be seen below in Figures 4.9 and 4.10.

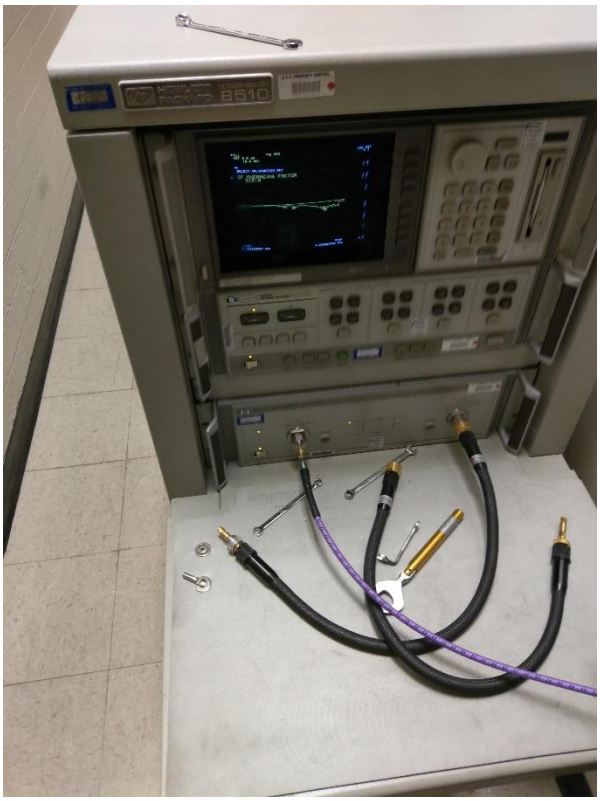

Figure 4.9 Experimental setup from the HP 8510 VNA

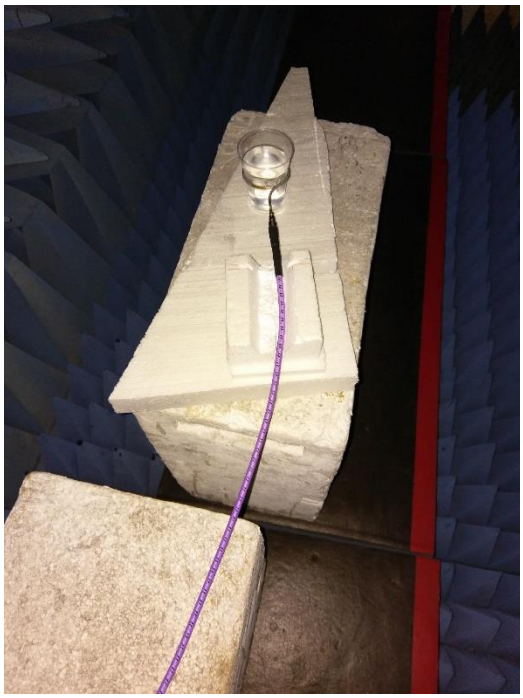

Figure 4.10 Setup inside the anechoic chamber with water inside the cup

The measurements were redone for both the shielded loop antenna in free space, and surrounding a plastic cup filled with distilled water. Like before, the measured data was converted to a *.s1p file and imported into ADS. The results from the free space measurements are shown below in Figures 4.11 and 4.12.

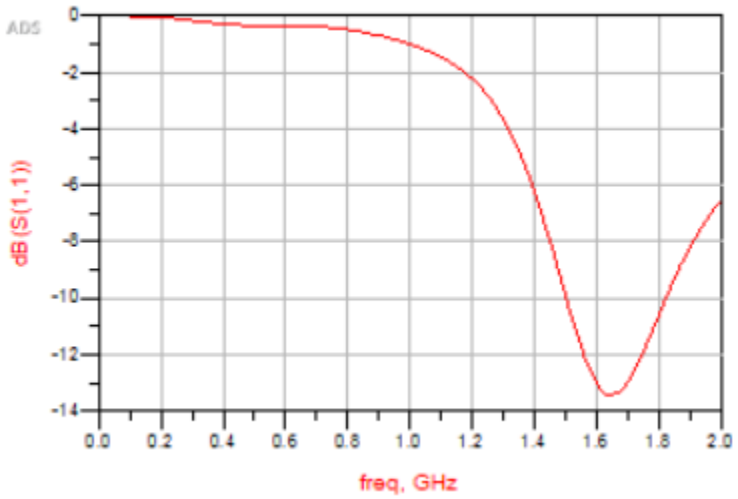

Figure 4.11 S(1,1) in dB of an empty cup from the anechoic chamber

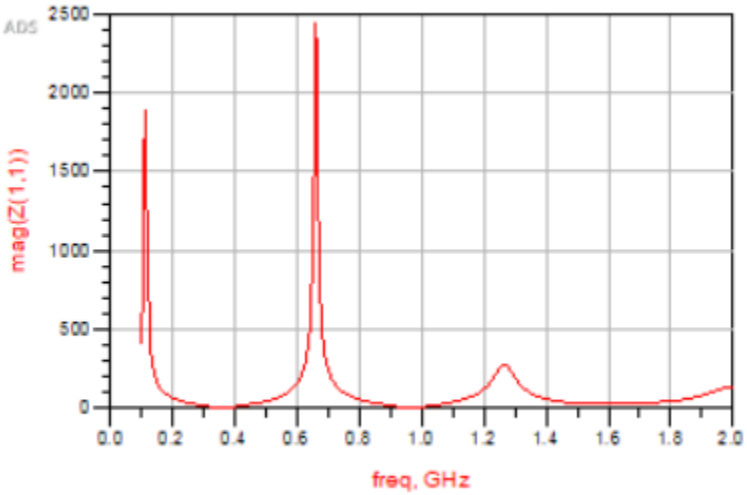

Figure 4.12 Z(1,1) in magnitude of an empty cup from the chamber

The measurements with a cup of distilled water are seen below in Figures 3.13 and 3.14.

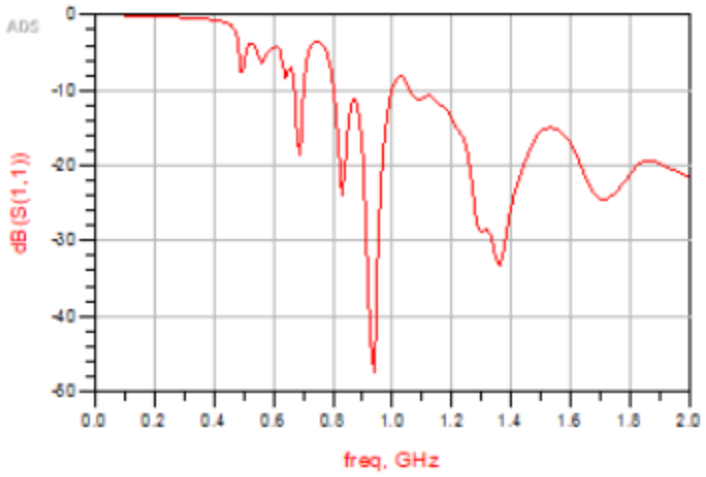

Figure 4.13 S(1,1) in dB of a cup of distilled water from the chamber

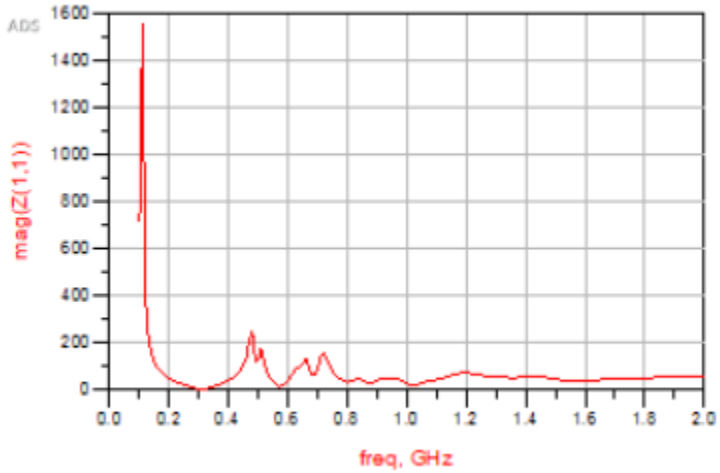

Figure 4.14 Z(1,1) in magnitude of a cup of distilled water from the chamber

This measured data is noticeably different than the theoretical (comparison seen below in Figures 4.15, 4.16, 4.17, and 4.18), but this difference may largely result from the assumptions regarding the plastic cup and the non-cylindrical shape of the water playing a minimal role.

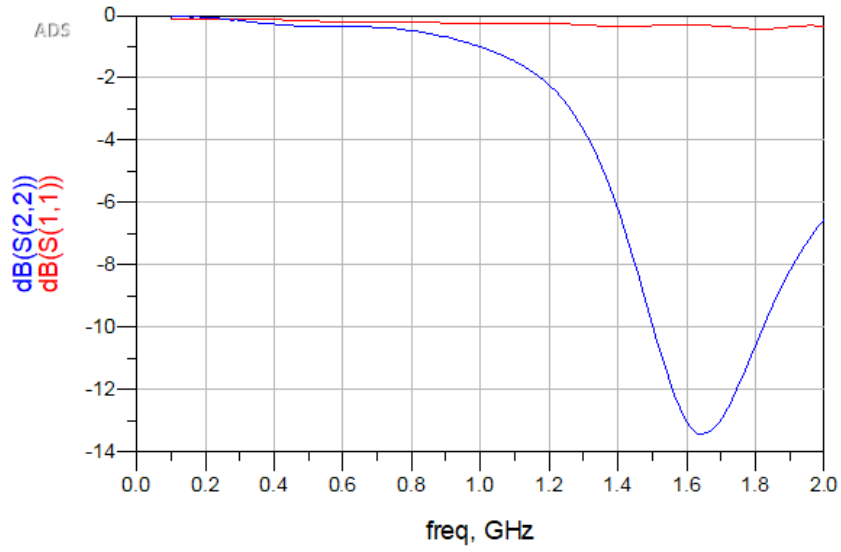

Figure 4.15 Reflected power in dB of free space. S(1,1) is theoretical, S(2,2) is measured

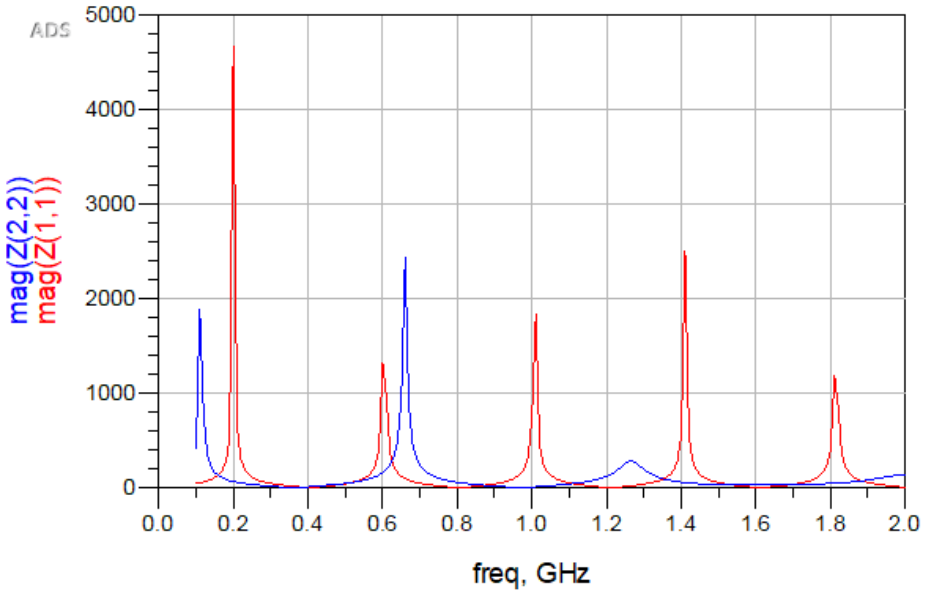

Figure 4.16 Input impedance in magnitude of free space. Z(1,1) is theoretical, Z(2,2) is measured

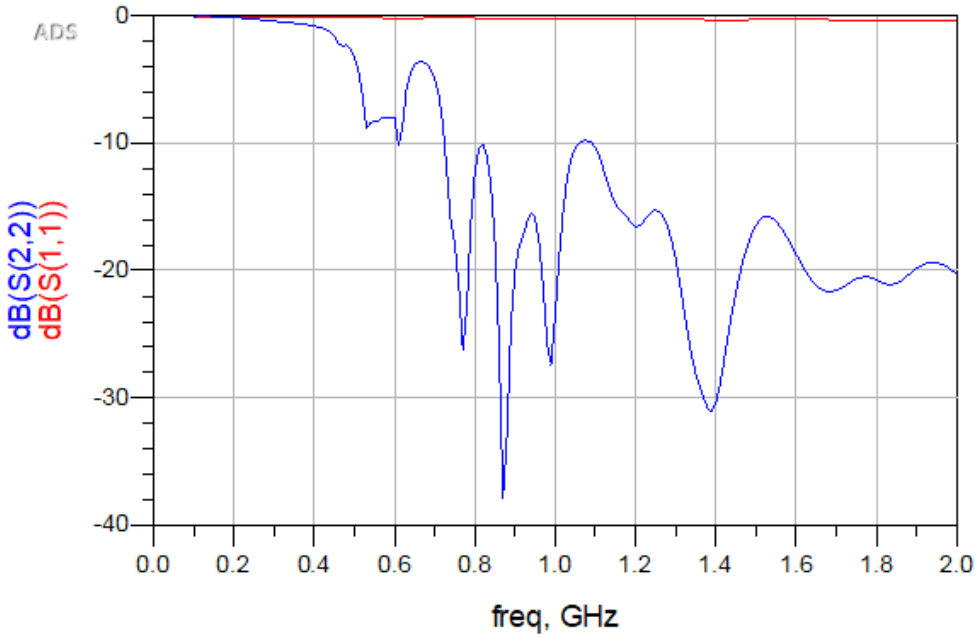

Figure 4.17 Reflected power in dB of distilled water. S(1,1) is theoretical, S(2,2) is measured

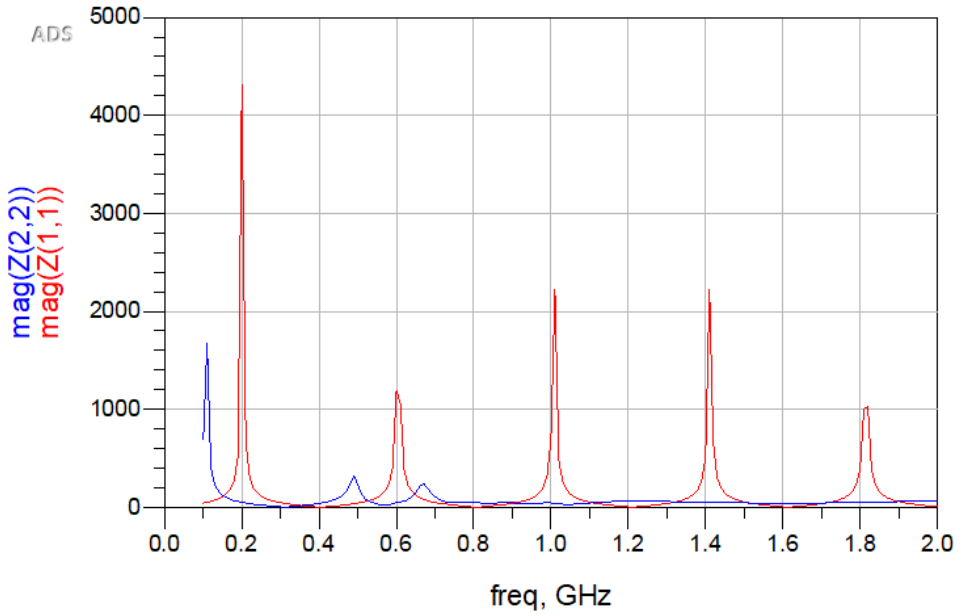

Figure 4.18 Input impedance in magnitude of distilled water. Z(1,1) is theoretical, Z(2,2) is measured

As seen from the comparison figures, the HFSS simulations do not agree enough to the measured data to allow simulated data to be used to predict the properties of the material under test. In the remainder of this thesis, an approach to determine the properties of a material under test using a calibration scheme based on measured data is described.

Calibration of Saline Solutions

To measure complex dielectrics, saline solutions with different molarity were used. These solutions exhibit complex dielectric constants and represent a decrease in the relative dielectric constant, as seen in Figure 4.19 below [7].

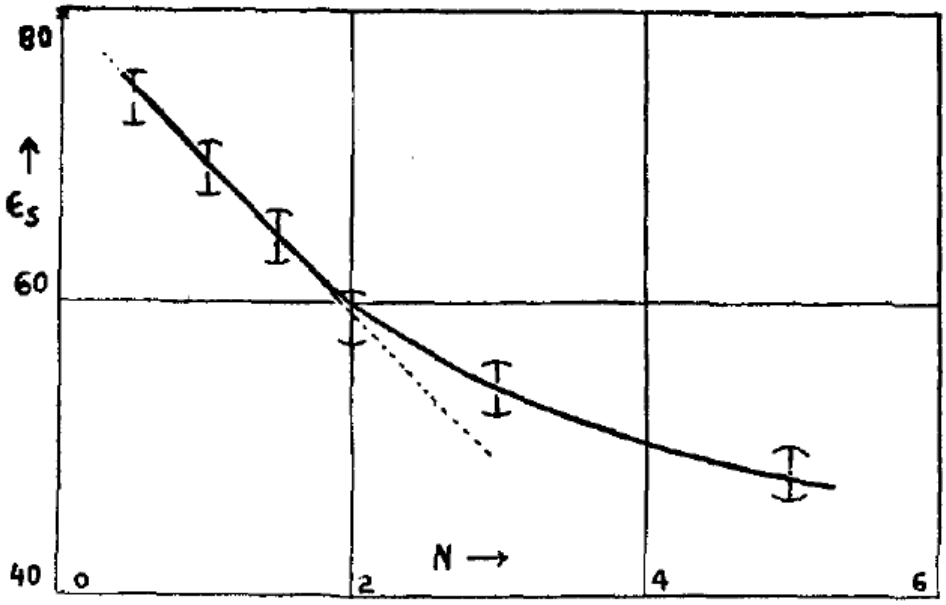

Figure 4.19 Static dielectric constant of NaCl solution plotted against normality N [7]

Note that while Gavish and Promislow use normality, the soluble solution of Na^+ and Cl^- have a 1:1 acid to base ratio, and thus normality is equivalent to molarity here. The dielectric of each molar solution can be approximated from the graph and is given in the table below.

Table 4.1 Approximate relative dielectric based on molarity

Desired Molarity	NaCl (grams)	Distilled Water (L)	Calculated Molarity (M)	Approximate Dielectric (Er)*
0M	0	0.2	0	80
1M	11.77	0.2	1.01	70
2M	23.38	0.2	2.00	60
3M	35.17	0.2	3.01	55
4M	46.75	0.2	4.00	51
5M	58.52	0.2	5.01	48

Another note is that the dielectric constant here is approximated. A more rigorous approach involving molarity is described in Chapter 5.

Each of these solutions was also tested in the anechoic chamber and the results were imported into ADS, with S(1,1) and Z(1,1) shown in Figures 4.20 and 4.21 respectively.

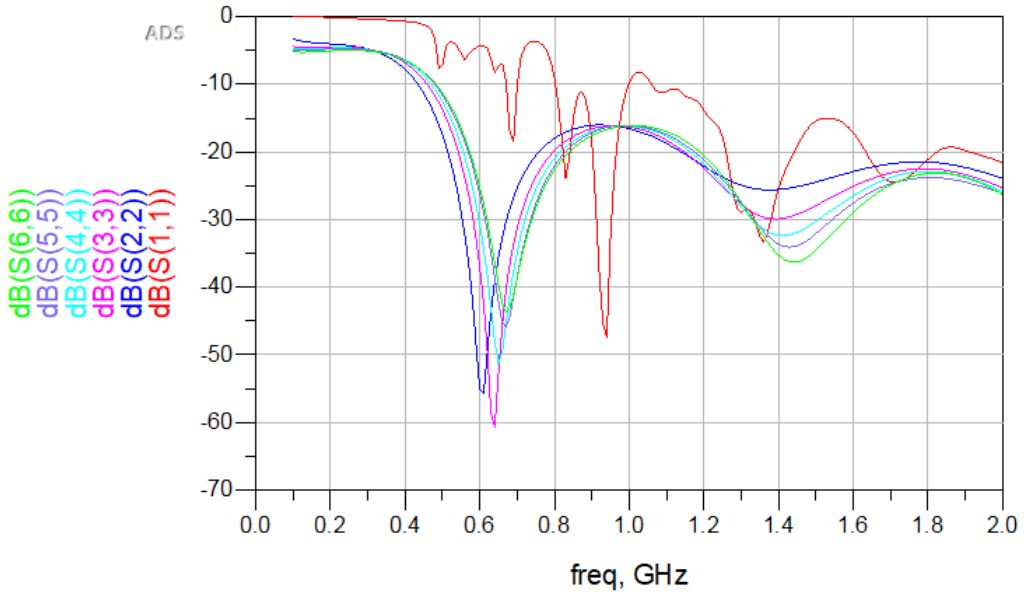

Figure 4.20 Frequency sweep of the return loss in dB. S(1,1) is the 0M solution; S(2,2), 1M; S(3,3), 2M; S(4,4), 3M; S(5,5), 4M; and S(6,6), 5M

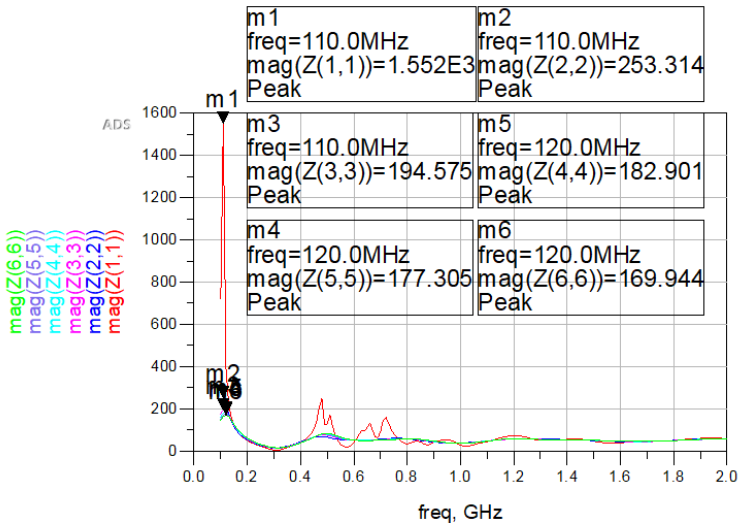

Figure 4.21 Frequency sweep of the input impedance in magnitude with each peak marked. Z(1,1) is the 0M solution; Z(2,2), 1M; Z(3,3), 2M; Z(4,4), 3M; Z(5,5), 4M; and Z(6,6), 5M.

The subtle differences between the different molar solutions are not apparent because of the overall magnitude of the reflection coefficient of the distilled water. The real and imaginary parts of the input impedance are shown below in Figures 4.22 and 4.23, with frequencies of the max peak in the magnitude marked.

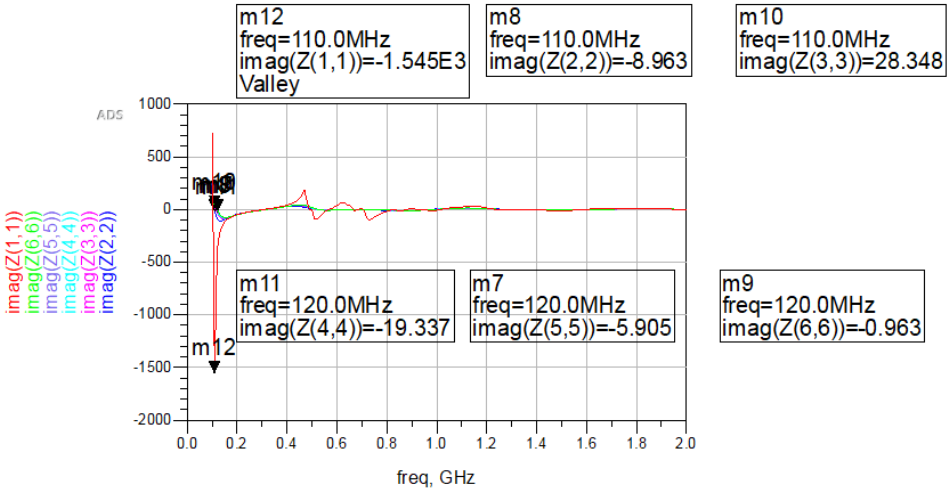

Figure 4.22 Frequency sweep of the imaginary part of the input impedance in magnitude with each peak marked. Z(1,1) is the 0M solution; Z(2,2), 1M; Z(3,3), 2M; Z(4,4), 3M; Z(5,5), 4M; and Z(6,6), 5M

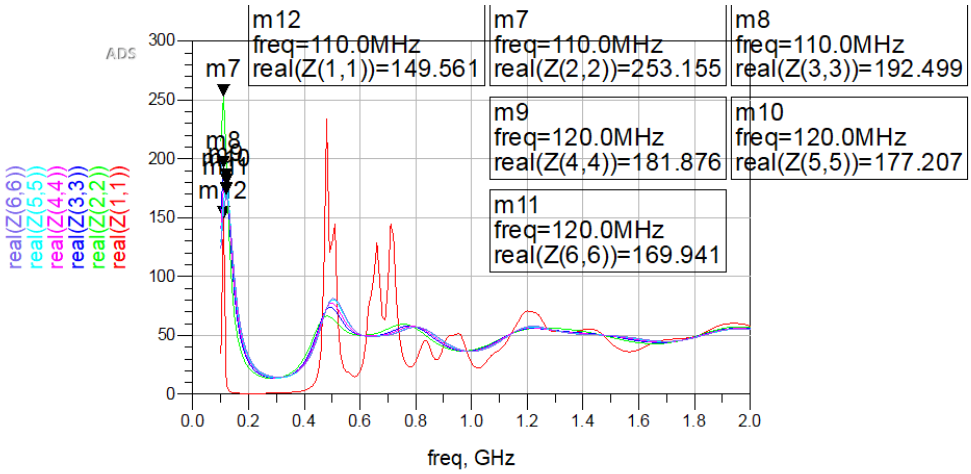

Figure 4.23 Frequency sweep of the real part of the input impedance in magnitude with each peak marked. Z(1,1) is the 0M solution; Z(2,2), 1M; Z(3,3), 2M; Z(4,4), 3M; Z(5,5), 4M; and Z(6,6), 5M

Overall, the trend of a lower input impedance is a lower peaking, as well as a slight increase in the frequency which the peaking occurs.

Testing Unknown Solutions

The final experiment was a black-box experiment in which another graduate student mixed solutions with an unknown molarity. The first set of these solutions were tested and the results are shown below in Figures 4.24 to 4.27.

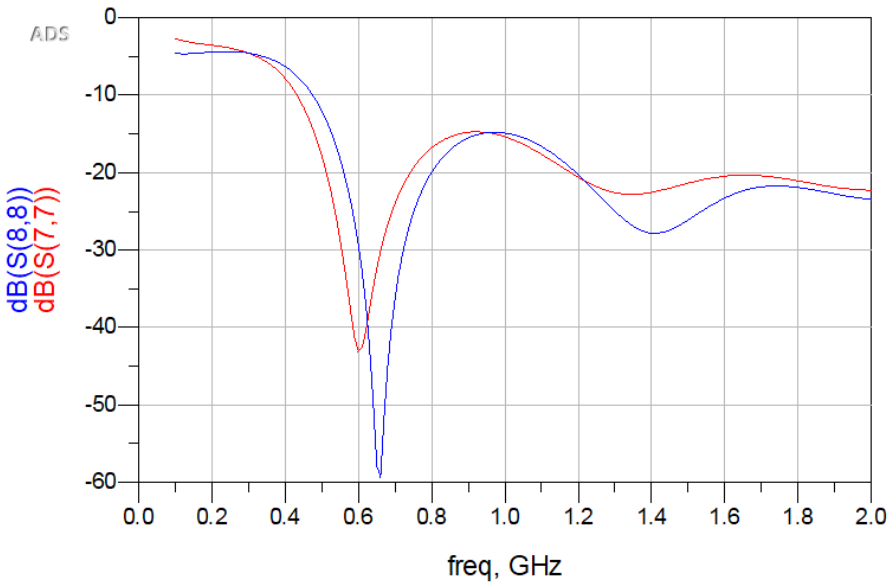

Figure 4.24 Frequency sweep of the return loss in dB for both unknown samples

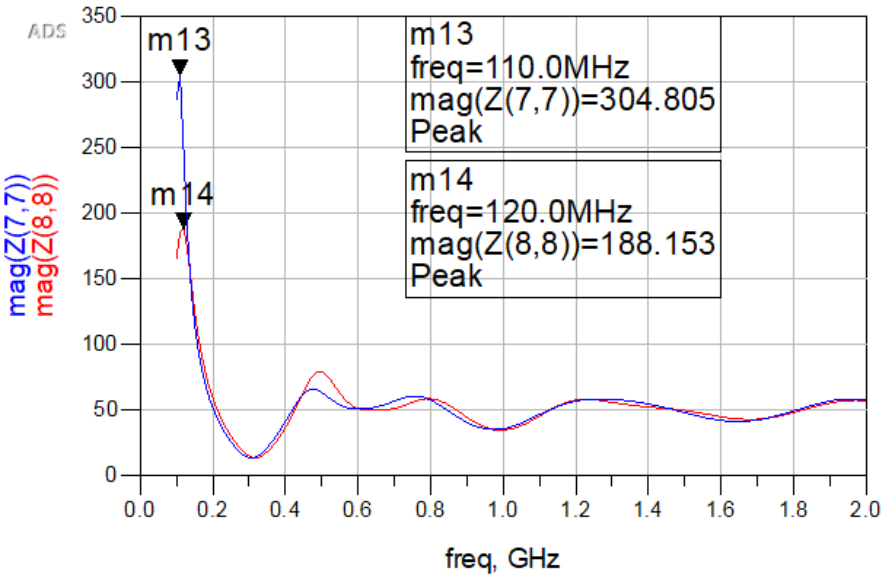

Figure 4.25 Frequency sweep of the input impedance in magnitude with each peak marked for both unknown samples

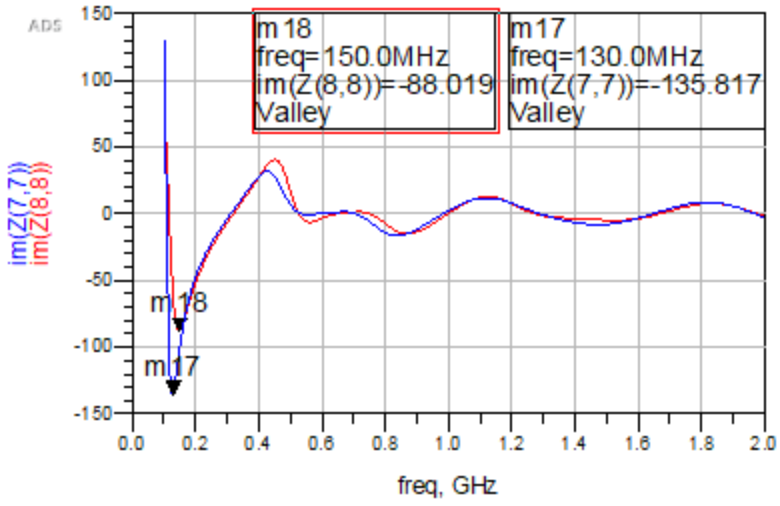

Figure 4.26 Frequency sweep of the imaginary part of the input impedance in magnitude with each peak marked for both samples

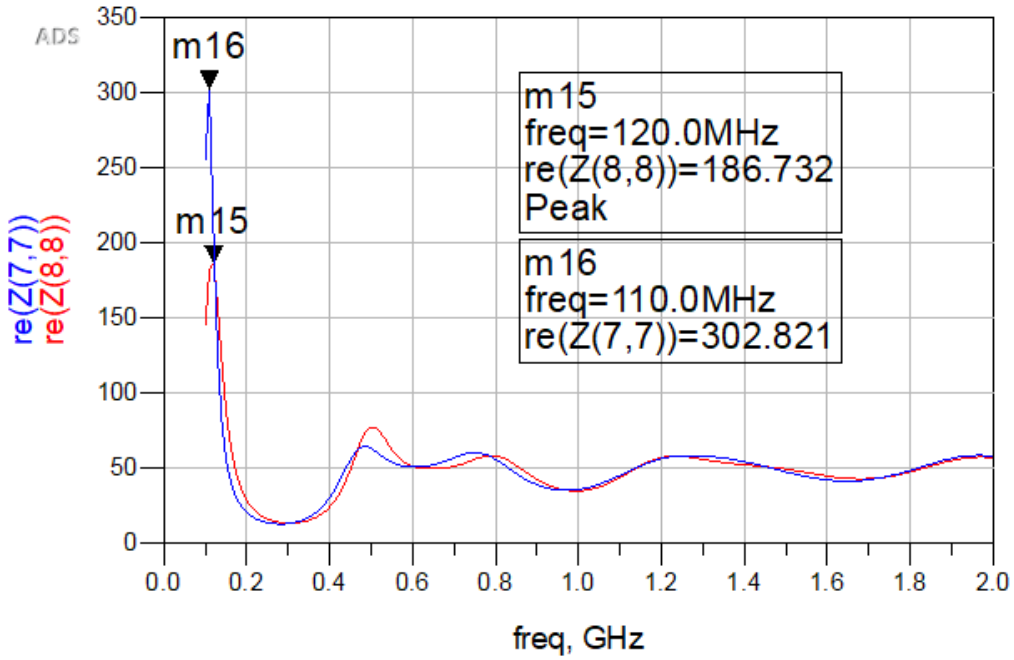

Figure 4.27 Frequency sweep of the real part of the input impedance in magnitude with each peak marked for both samples

Simply looking at the magnitude value is enough to find the range of molarities that each unknown solution is. The first unknown (marked as 7 on the simulation result) has a peak input impedance of 304.8 ohms, and the second unknown (marked as 8 on the

simulation result) has a peak input impedance of 188.2 ohms. The molarity of the first solution was not able to be found accurately, as this unknown sample had a molarity that was under 1M. As the reflection coefficient of distilled has a different profile than that of saline solutions, there was not enough points under 1M to accurately find the molarity, because the trend is logarithmic (as detailed in Chapter 5). The other unknown solution was in the range of 2M and 3M. Using the data post-analysis from the known solutions (seen in Chapter 4), the molarity was approximated at 2.5M. The actual molarity was later revealed to be 2.5M, which is close (wrong only by non-significant figures).

Second Set of Saline Solutions for Calibration

Because one of the solutions was not able to be found, another set of known solutions with molarities ranging from 0.2M to 1.8M were tested to extend the calibration data and successfully solve for the unknown. The second set of solution measurements is seen below in Figures 4.28 through 4.31.

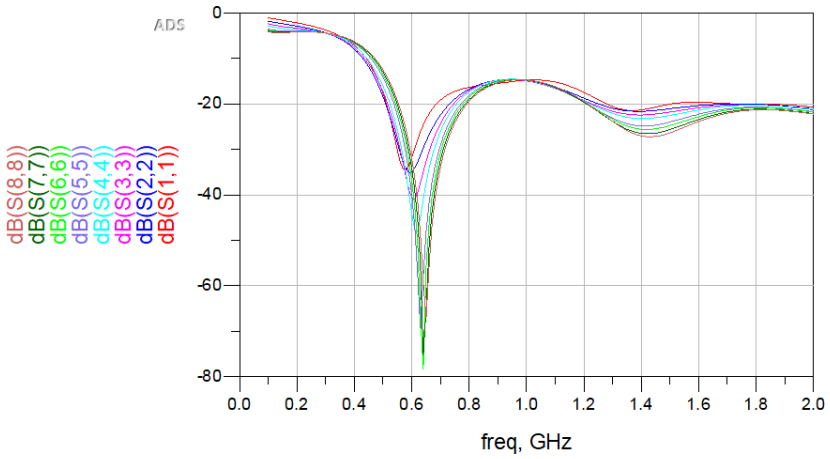

Figure 4.28 Frequency sweep of the return loss in dB. S(1,1) is the 0.2M solution; S(2,2), 0.4M; S(3,3), 0.6M; S(4,4), 0.8M; S(5,5), 1.2M; S(6,6), 1.4M; S(7,7), 1.6M; and S(8,8), 1.8M

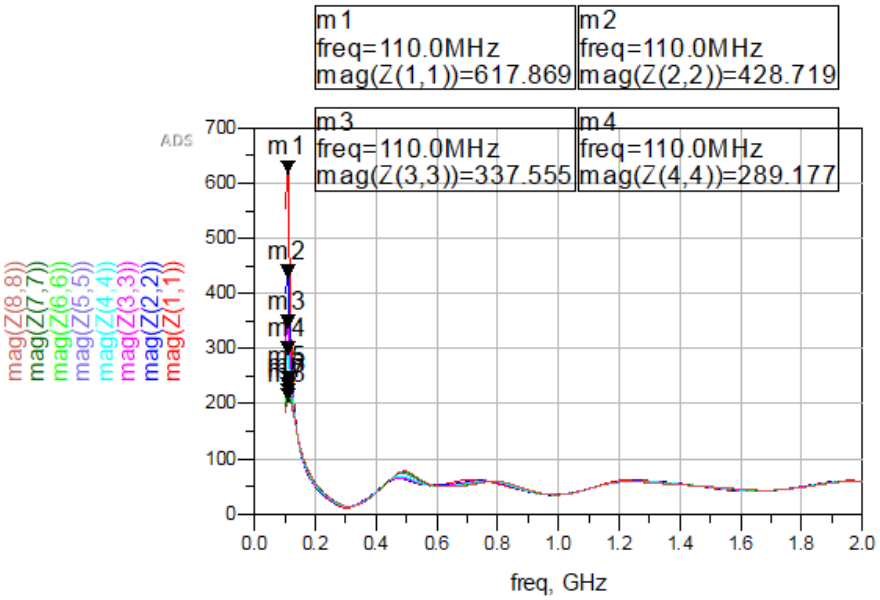

Figure 4.29a Frequency sweep of the input impedance in magnitude with each peak marked. Z(1,1) is the 0.2M solution; Z(2,2), 0.4M; Z(3,3), 0.6M; and Z(4,4), 0.8M

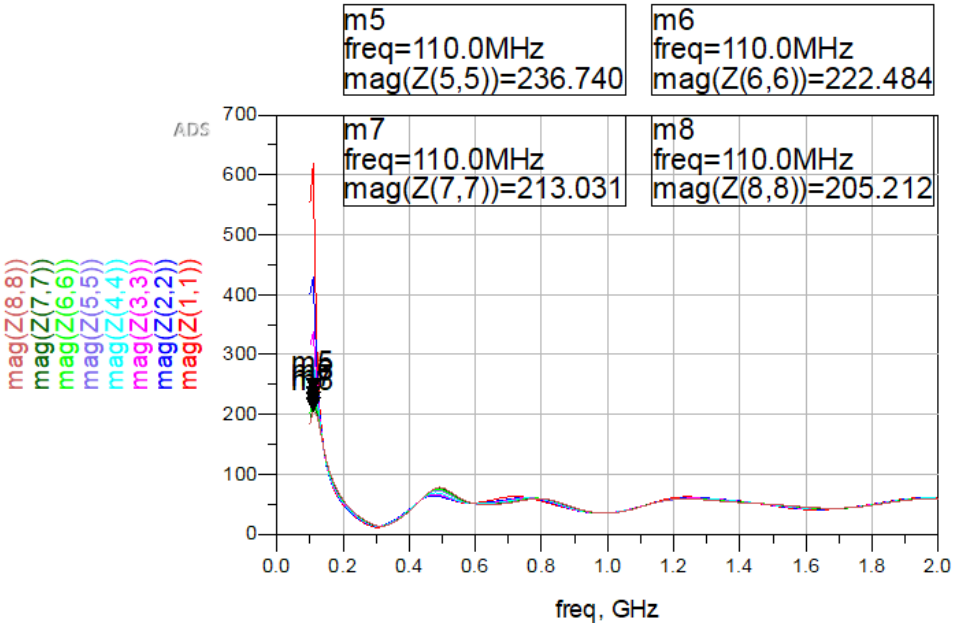

Figure 4.29b Z(5,5) is the 1.2M solution; Z(6,6), 1.4M; Z(7,7), 1.6M; and Z(8,8), 1.8M

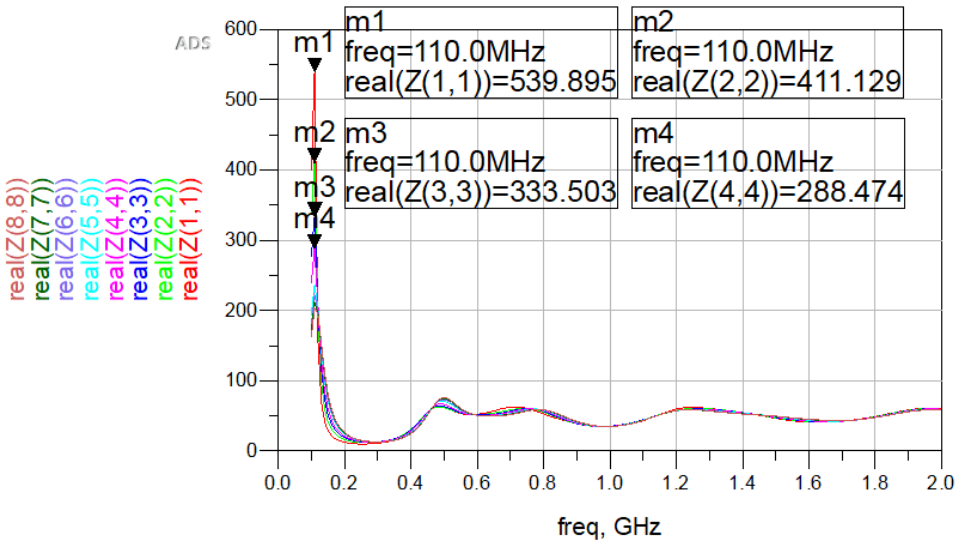

Figure 4.30a Frequency sweep of the real part of the input impedance in magnitude with each peak marked. Z(1,1) is the 0.2M solution; Z(2,2), 0.4M; Z(3,3), 0.6M; and Z(4,4), 0.8M

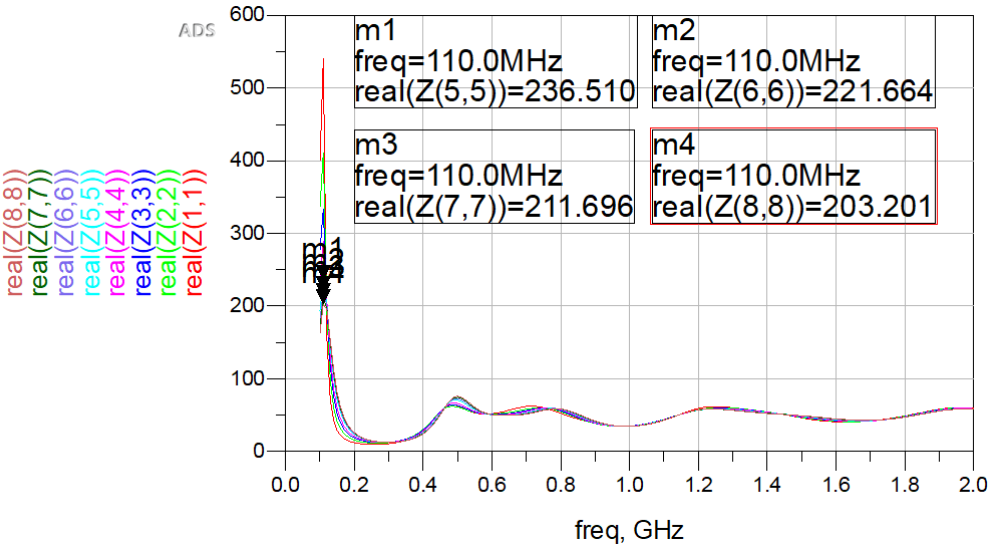

Figure 4.30b Z(5,5) is the 1.2M solution; Z(6,6), 1.4M; Z(7,7), 1.6M; and Z(8,8), 1.8M

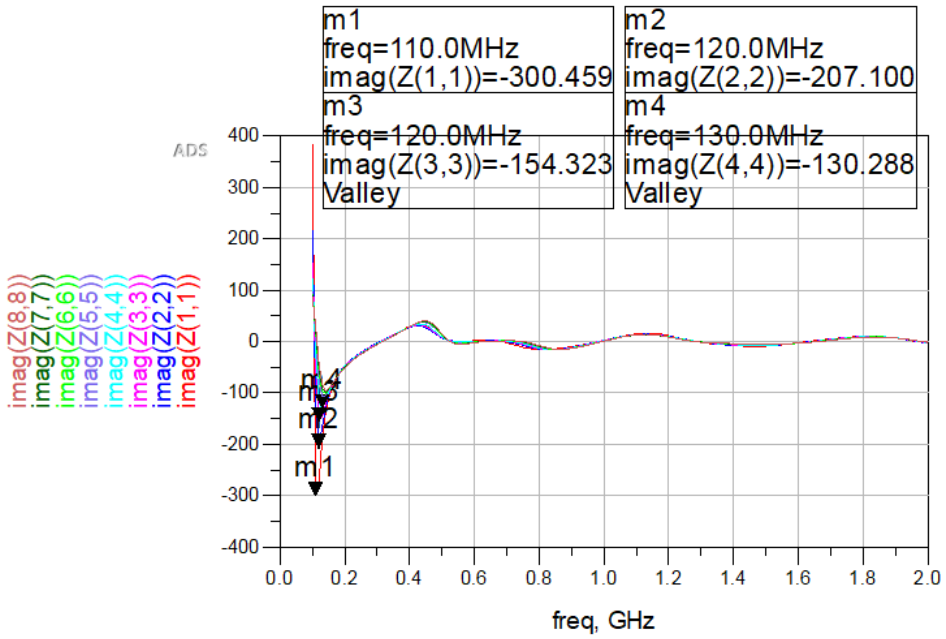

Figure 4.31a Frequency sweep of the real part of the input impedance in magnitude with each peak marked. Z(1,1) is the 0.2M solution; Z(2,2), 0.4M; Z(3,3), 0.6M; and Z(4,4), 0.8M

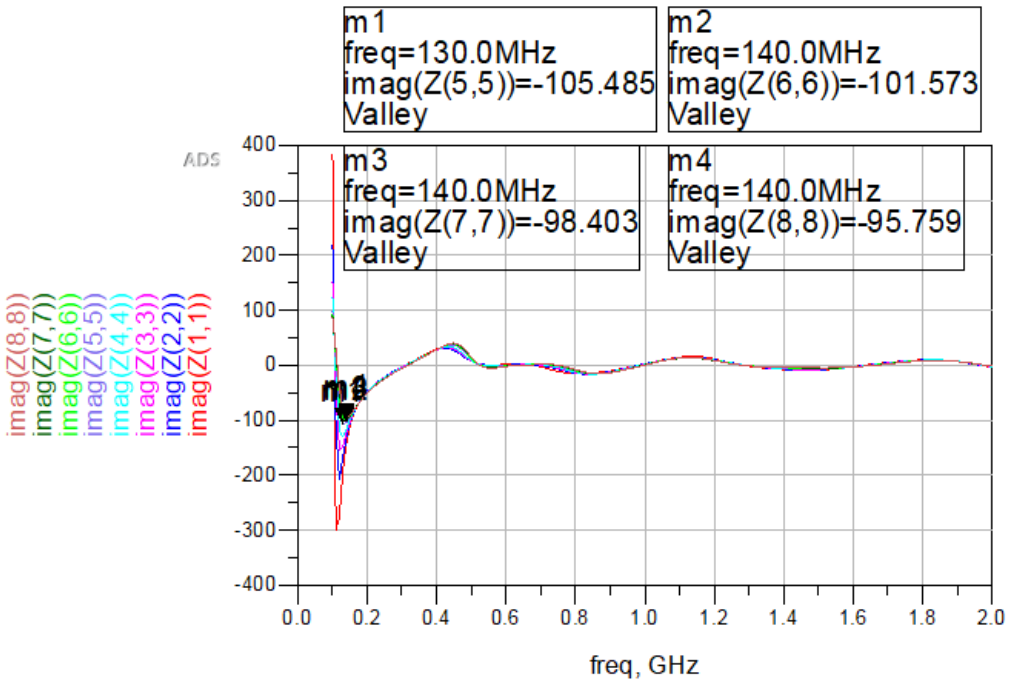

Figure 4.31b Z(5,5) is the 1.2M solution; Z(6,6), 1.4M; Z(7,7), 1.6M; and Z(8,8), 1.8M

The new data points are enough to increase the logarithmic trend in the approximate region to find the first unknown. As aforementioned, the unknown has a peak input impedance of 304.8 ohms. Using the data post-analysis from the known solutions (seen in Chapter 5), the molarity was approximated at 0.7M. The actual molarity was later revealed to be 0.7M, which again is only off by non-significant figures.

Continuation of Unknown Solution Testing

Following this set, the other graduate student mixed another set of 3 unknowns to be tested. The second set of were tested, and the results are shown below in Figures 4.32 to 4.35.

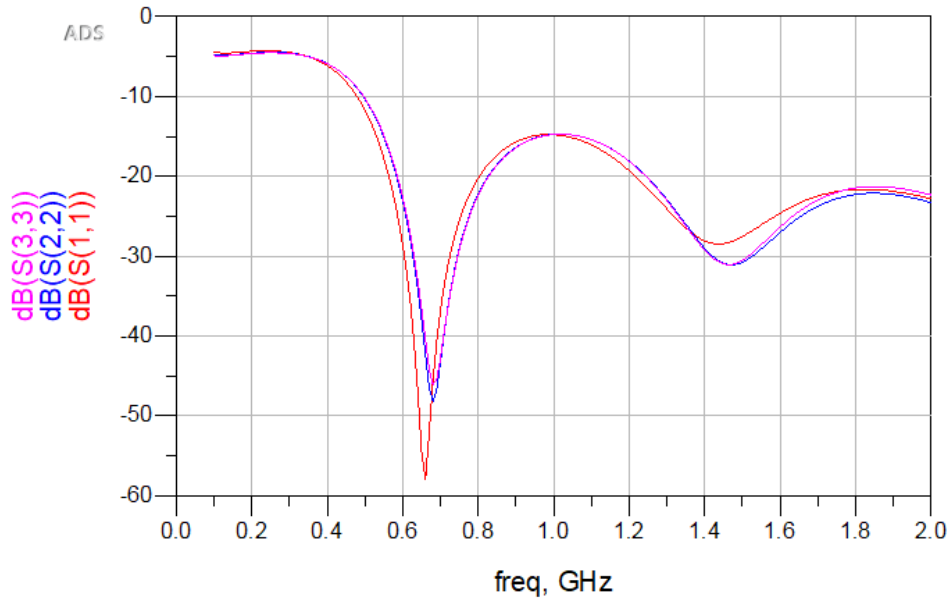

Figure 4.32 Frequency sweep of the return loss in dB for three unknown samples

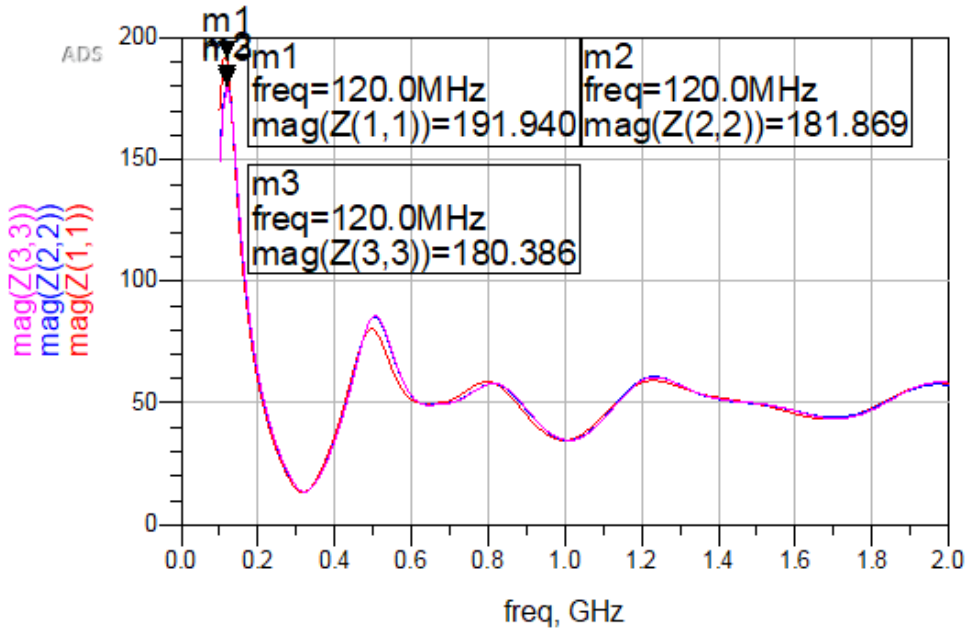

Figure 4.33 Frequency sweep of the input impedance in magnitude with each peak marked for the three unknown samples

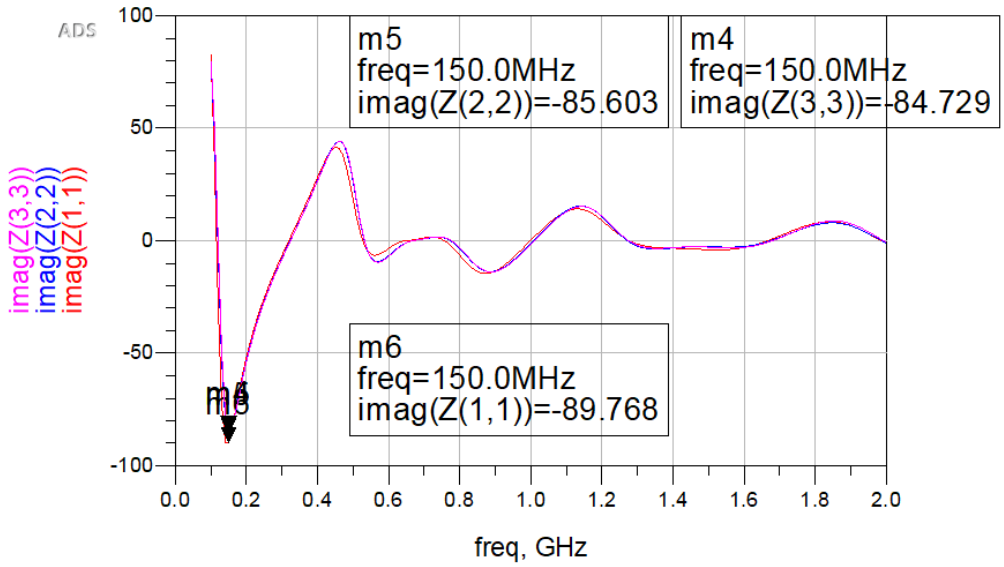

Figure 4.34 Frequency sweep of the imaginary part of the input impedance in magnitude with each peak marked for the three samples

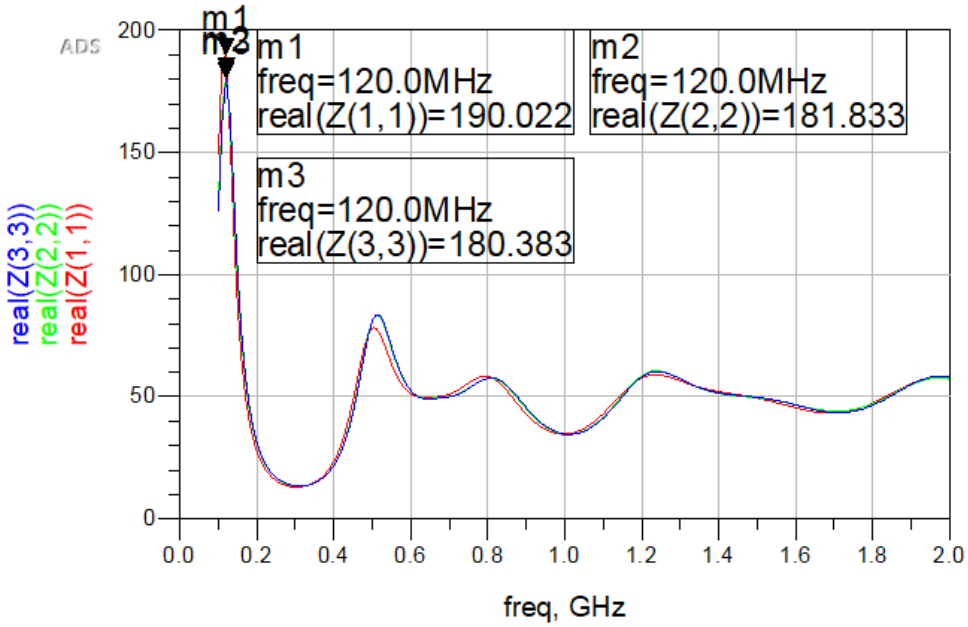

Figure 4.35 Frequency sweep of the real part of the input impedance in magnitude with each peak marked for the three samples

Again, using the magnitude value is enough to find the range of molarities that each unknown solution is. The first unknown (marked as 1 on the simulation result) has a peak input impedance of 190.0 ohms, the second unknown (marked as 2 on the simulation result) has a peak input impedance of 181.8 ohms, and the third unknown (marked as 3 on the simulation result) has a peak input impedance of 180.383. The first unknown solution was in the range of 2M and 3M. Using the data post-analysis from the known solutions (seen in Chapter 4), the molarity was approximated at 2.2M. The actual molarity was later revealed to be 2.2M, which again is close and only off by non-significant figures. Both the second and the third unknown were in the range of 3M and 4M. The molarity of the second and the third unknowns were approximated to be 3.2M and 3.4M respectively. These were later revealed to be 3.7M and 4.3M.

Reconciliation between Estimates and Actual Data

While it seems that these results are somewhat inaccurate, this phenomenon can be reasonably explained. With the original set of solutions that were tested, a range of 1M to 6M was actually desired. However, because the 6M was not able to be dissolved completely into the distilled water, the 6M solution was not tested at all, because there was no guarantee of the actual molarity of the solution. This phenomenon occurred with lab-grade sodium chloride (no additives). When the graduate student mixed the solutions for testing, lab-grade salt was not used, but rather ordinary table salt was used. Ordinary table salt is iodized, meaning the salt is covered with iodine in some way. This change seems to influence the solubility of the salt in the saline solution. Both the second and the third unknown samples had salt residue in the beaker. A picture of the third sample is provided (in Figure 4.36) with the saline solution tipped to show the salt both in the water and the salt left in the beaker.

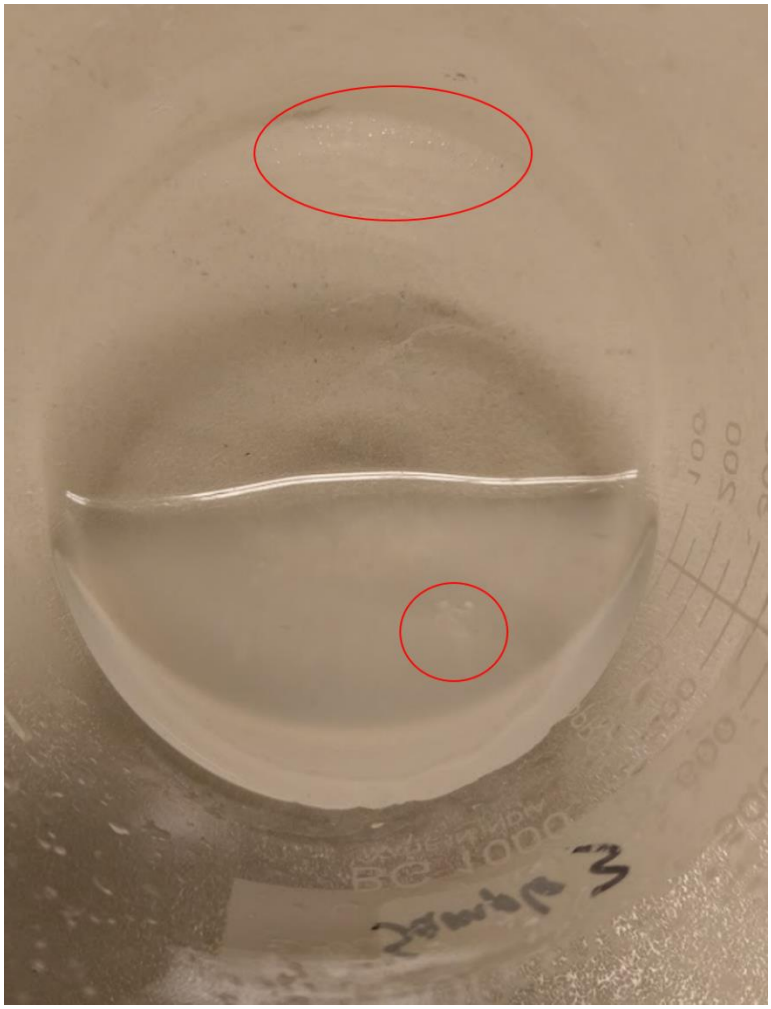

Figure 4.36 Sample 3 with salt residue circled

To underscore this phenomenon, a mixture of 4.25M with lab grade salt was mixed and a comparison photo can be seen below in Figure 4.37.

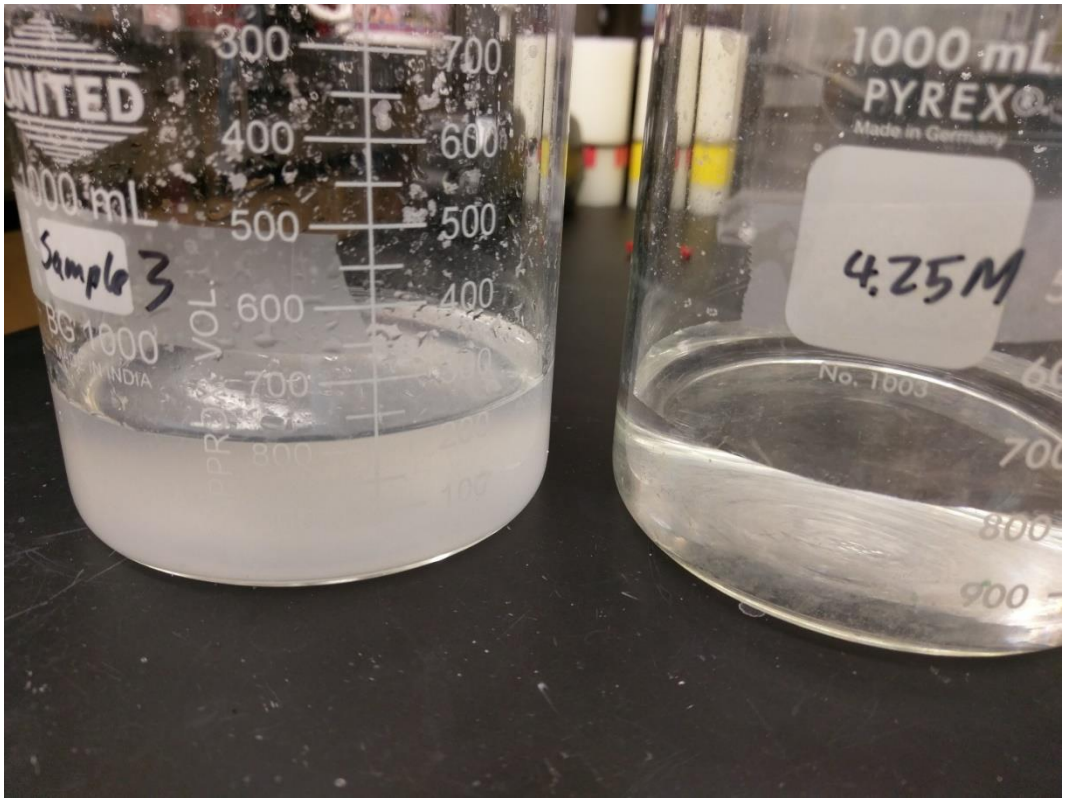

Figure 4.37 Sample 3, a 4.3M table salt solution (left) and a 4.25M lab-grade salt solution (right)

As seen here, the 4.25M solution is nearly transparent, while sample 3 is translucent at best. It seems reasonable that the solubility of the table salt is not as high as lab grade salt and is the main cause for the mischaracterized solutions. Though there was enough salt added into the unknown samples for the calculated molarity, the actual molarity of these solutions is lower, because these solutions have almost hit the solubility limit, just like the 6M solution with the lab grade salt.

Characterization of Table Salt and Lab Grade Salt

For validation that the iodized table salt and lab grade table salt actually have the same characteristics at lower frequencies, another set of solutions was tested. Both of

these solutions were roughly 1.5M, but one was made with lab grade salt and the other with iodized table salt. A photo of these two solutions is seen below in Figure 4.38.

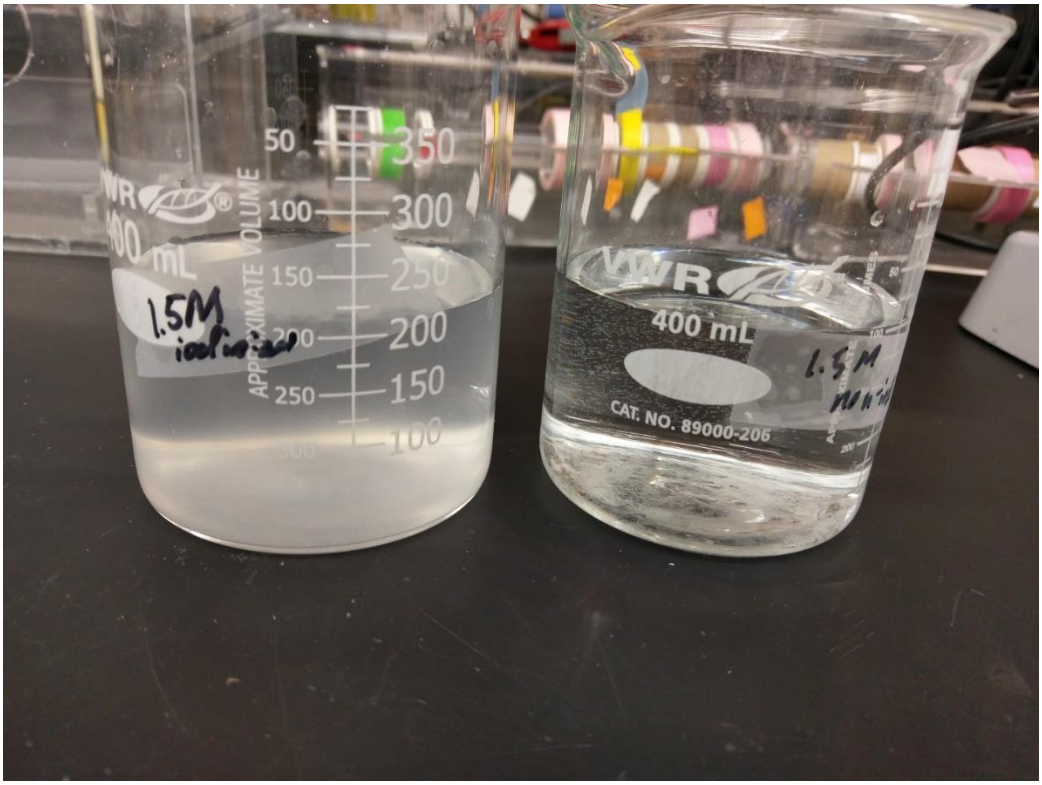

Figure 4.38 A 1.5M table salt solution (left) and a 1.5M lab-grade salt solution (right)

The difference of iodized salt and lab-grade salt with regards to solubility is apparent not just in transparency but also time. The 1.5M solution of table salt took longer than the 4.25M lab grade salt to mix, despite being mixed with the same beaker and magnetic stirrer (both cleaned and dried in between solutions). The increased time to dissolve the salt underscores the lack of solubility in iodized table salt.

The two solutions with roughly the same molarity were tested, and the results are shown in Figures 4.39 to 4.42.

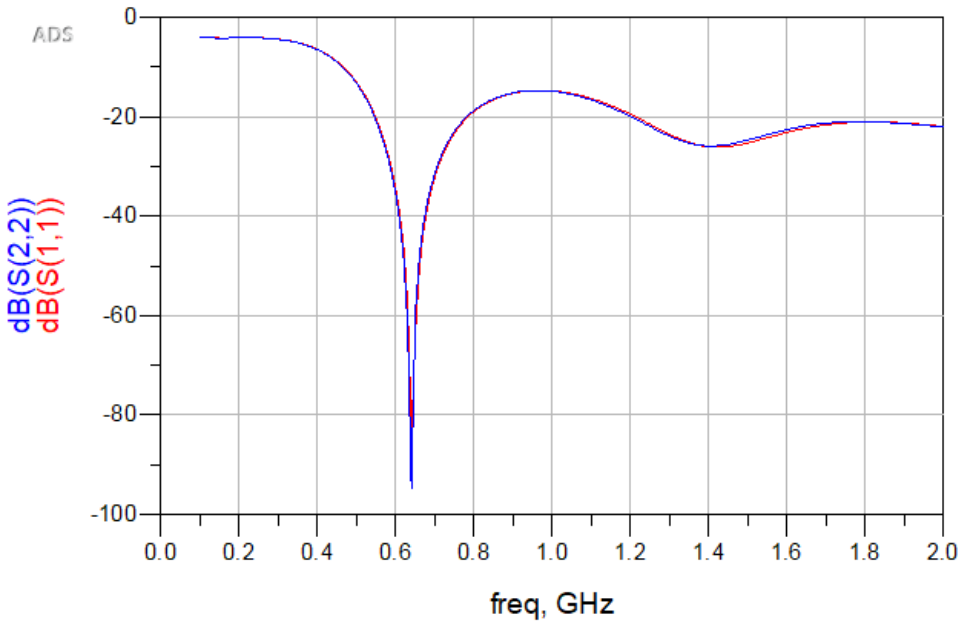

Figure 4.39 Frequency sweep of the return loss in dB for the 1.5M solutions

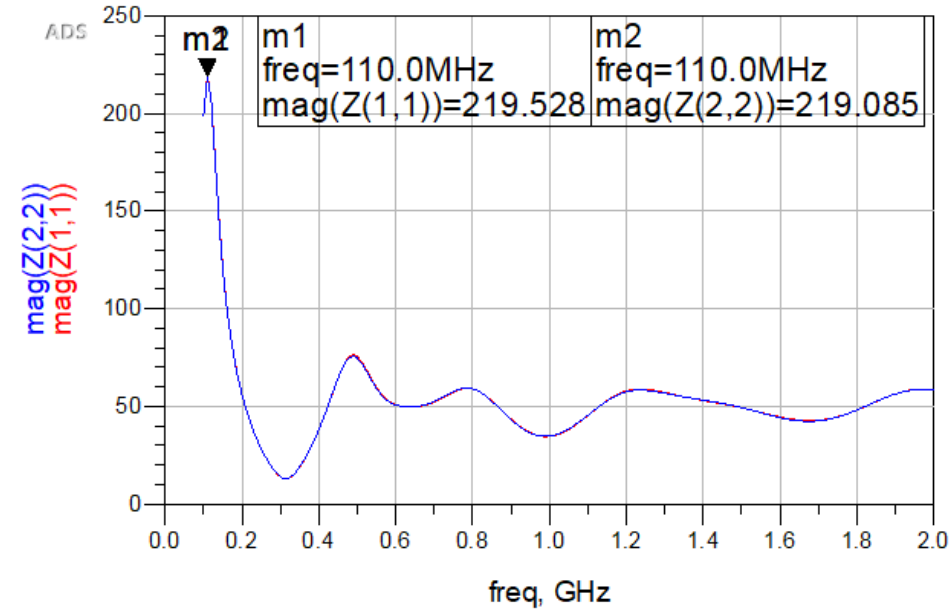

Figure 4.40 Frequency sweep of the input impedance in magnitude with each peak marked for the 1.5M solutions

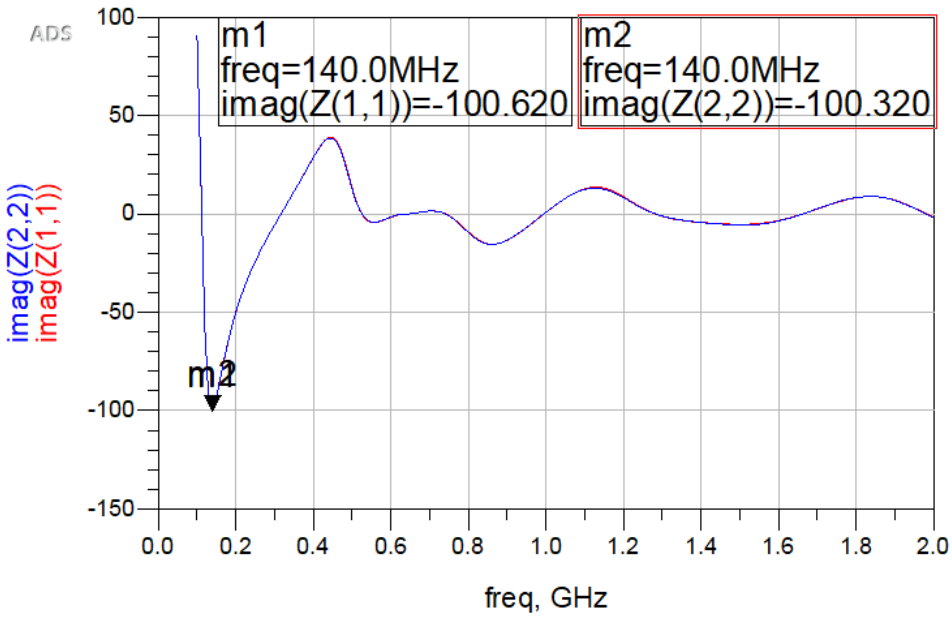

Figure 4.41 Frequency sweep of the imaginary part of the input impedance in magnitude with each peak marked for the 1.5M solutions

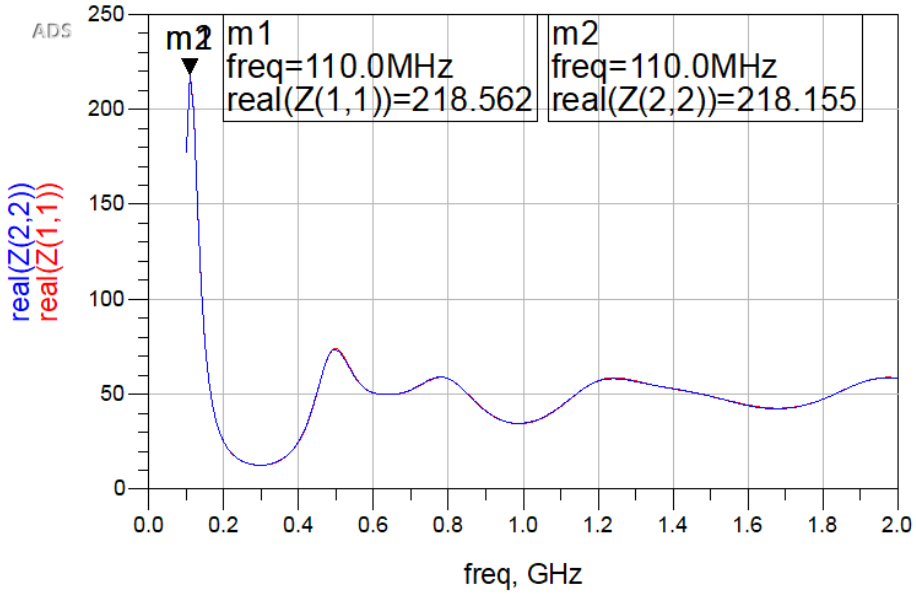

Figure 4.42 Frequency sweep of the real part of the input impedance in magnitude with each peak marked for the 1.5M solutions

The difference between the iodized salt and lab-grade salt with regards to the return loss and the input impedance is negligible at lower frequencies. The only

difference between lab grade salt and table salt can only be seen with regards to solubility, not the actual measurement of the dielectric given that the solute is completely dissolved. The final black-box experiment is therefore valid.

CHAPTER 5

DATA ANALYSIS AND DISCUSSION

Trends for Estimation

A plot was created using the known measurements of the approximate solutions of 1M to 5M and the magnitude of the input impedance, shown in Figure 5.1.

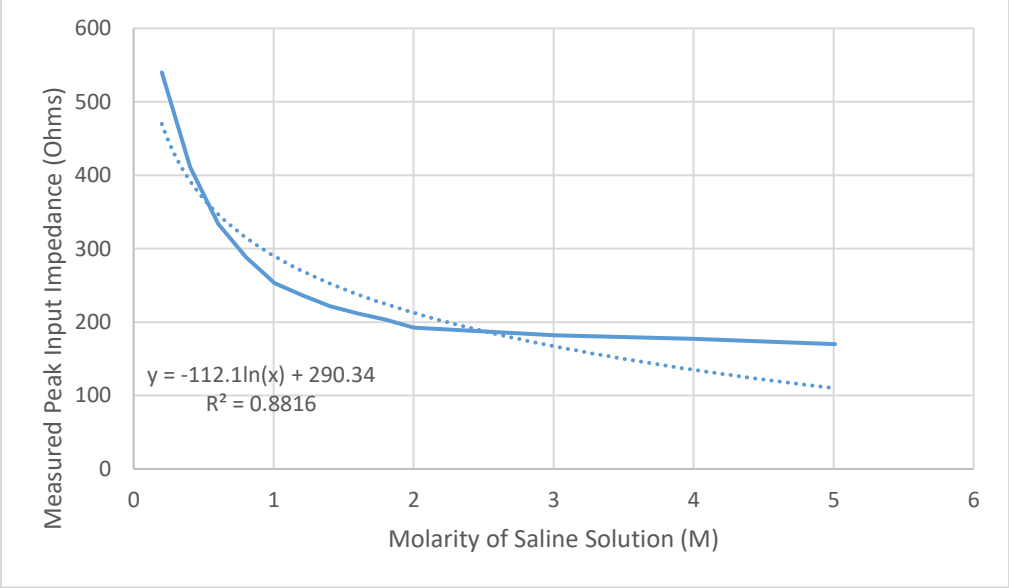

Figure 5.1 All saline solutions (M) plotted against measured peak magnitude of input impedance

From Figure 5.1, the general trend is very clearly logarithmic. However, the line of best fit does not give a very good approximation for finding values, so a more detailed analysis of how to divide the data and develop appropriate approximations over each subinterval is necessary.

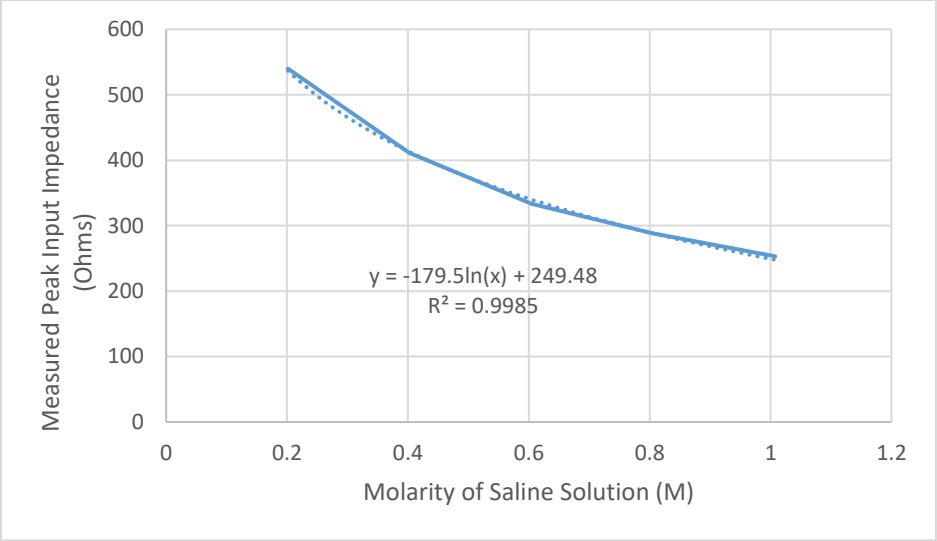

Figure 5.2 Saline solutions (0.2M to 1M) plotted against measured peak magnitude of the input impedance

This trend line was used to approximate the value of the second unknown from first set of black-box tests. However, the trend line shown here is only valid for molarities under 1M solutions. By increasing the overall trend from 0.2M to 2M yields another trend line, as seen in Figure 5.3.

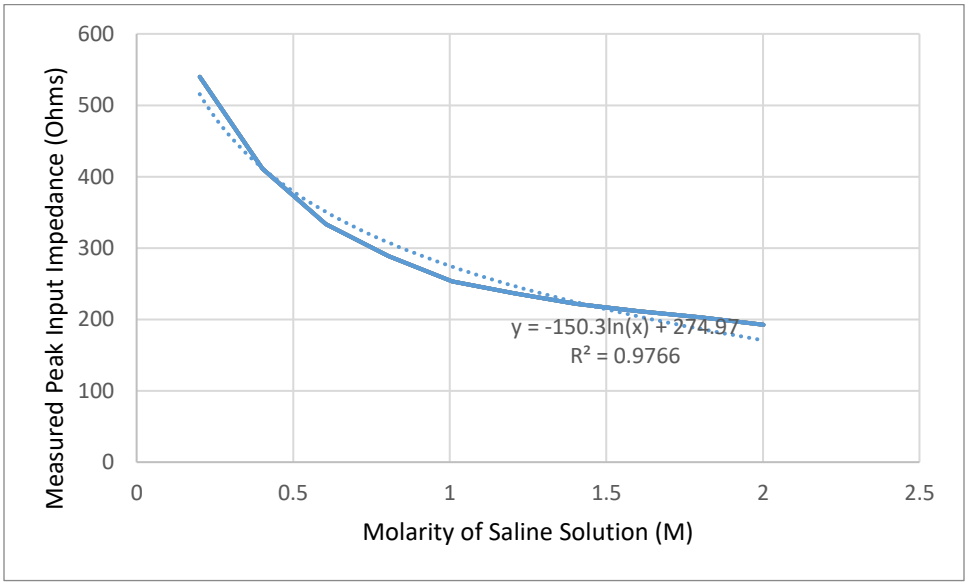

Figure 5.3 Saline solutions (0.2M to 2M) plotted against measured peak magnitude of the input impedance

This trend line was used to approximate the value of the first unknown from first set of black-box tests. However, the trend line shown here begins to diverge from the actual results. Without more data points from 2M to 5M, the best approach to approximate the molarities is to add another trend line from 2M to 5M. From Figure 5.1, it seemed reasonable to approach this section of the graph with a linear regression line first, then see how a logarithmic line would fit, shown in Figures 5.4a and 5.4b.

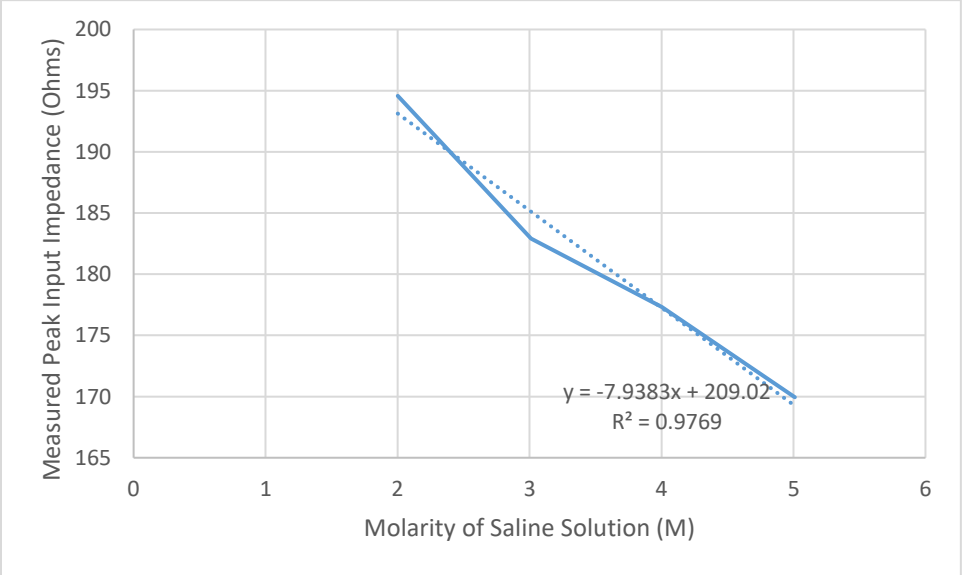

Figure 5.4a Saline solutions (2M to 5M) plotted against measured peak magnitude of the input impedance with a linear trend line

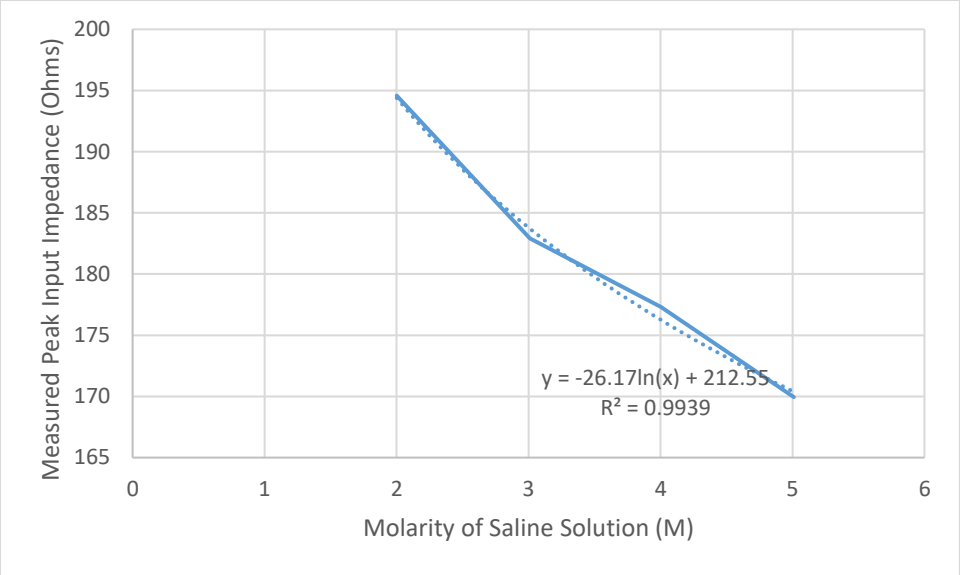

Figure 5.4b Saline solutions (2M to 5M) plotted against measured peak magnitude of the input impedance with a logarithmic trend line

As seen here, the logarithmic fits better than the linear, but not by much. This trend may also be largely caused by a lack of data points, so having more data points tested would give a much better trend line. The data from both these graphs were used to find the second set of solutions. The first unknown of the second set was approximated to be 2.15M with the linear fit, and 2.19 with the logarithmic fit; second unknown had 3.4M with the linear fit and 3.23M with the logarithmic fit; and the third had 3.607M with the linear and 3.418 with the logarithmic fit (within rounding error). The logarithmic fit was chosen to be the guess, as the logarithmic trend is the overall trend of the data.

Using Molarity to Calculate Permittivity

Salt saline solutions have a well-defined relationship between molarity and dielectric constants. The equations presented by Gavish and Promislow to predict the dielectric constant of saline solutions are shown below:

$$\varepsilon_s = \varepsilon_w - \alpha * c \quad (5\text{-}1)$$

This equation—where ε_s is the relative dielectric of the solution, ε_w is the relative dielectric of water, α is total excess polarization of the ionic species, and c is the concentration of the solution—is valid for dilute solutions (less than 2M). For equations greater than 2M, the following equation is used instead:

$$\varepsilon_s = \varepsilon_w - \beta * L\left(\frac{3\alpha c}{\beta}\right) \quad (5\text{-}2)$$

The L here is the Langevin function, defined below:

$$L(x) = \coth(x) - \frac{1}{x}$$

The β here is defined below:

$$\beta = \varepsilon_w - \varepsilon_{ms}$$

where ε_{ms} is the molten salt dielectric, the limiting dielectric constant for a non-dilute solution. The value ε_{ms} is directly related to solubility and therefore related to temperature [7].

Given these parameters, Gavish and Promislow have already defined values of α and β for a temperature of 25°C, 11.5 and 47.95 respectively. Gavish and Promislow also demonstrated that using the following first order approximation of the Langevin,

$$L(x) \approx 1 - \frac{1}{x}$$

is valid and accurate [7]. Using these values, the following table with calculated dielectrics for all known solutions is given below (lab grade salt was used except when noted):

Table 5.1 Relative dielectric based on molarity

Desired Molarity	NaCl (grams)	Distilled Water (L)	Calculated Molarity (M)	Relative Dielectric (Er)
0M	0	0.2	0	80
0.2M	2.35	0.2	0.20	78.68
0.4M	4.70	0.2	0.40	76.37
0.6M	7.06	0.2	0.60	74.05
0.8M	9.40	0.2	0.80	71.75
1M	11.77	0.2	1.01	69.41
1.2M	14.08	0.2	1.21	67.13
1.4M	16.39	0.2	1.40	64.87
1.5M (table)	17.15	0.2	1.47	64.11
1.5M	17.15	0.2	1.47	64.11
1.6M	18.72	0.2	1.60	62.57
1.8M	21.03	0.2	1.80	60.30
2M	23.38	0.2	2.00	57.98
3M	35.17	0.2	3.01	54.20
4M	46.75	0.2	4.00	48.73
5M	58.52	0.2	5.01	45.38

The following table shows the values for the unknown solutions, and their approximate dielectric value:

Table 5.2 Dielectric values based on molarity for black-box experiment

Desired Molarity	NaCl (grams)	Distilled Water (L)	Calculated Molarity (M)	Relative Dielectric (Er)
0.7M	8.176	0.2	0.70	72.96
2.2M	25.696	0.2	2.20	63.80
2.5M	29.2	0.2	2.50	59.74
3.7M	43.216	0.2	3.70	51.10
4.3M	50.224	0.2	4.30	48.59

As aforementioned, the 3.7M and the 4.3M solutions did not fully dissolve the solute. While they are included in the table above, the following table, which shows the difference between calculated and estimated values, will neglect these two values:

Table 5.3 Comparison of the molarity and dielectric values

Calculated Molarity (M)	Relative Dielectric (Er)	Type of Regression	Best Estimate	Estimated Dielectric (Er)	Error
0.7M	72.96	Log	0.7M	72.55	-0.56%
2.2M	63.38	Linear	2.2M	64.06	1.07%
2.2M	63.38	Log	2.2M	63.36	-0.03%
2.5M	59.74	Linear	2.5M	59.41	-0.55%
2.5M	59.74	Log	2.5M	59.31	-0.72%

As seen above, the error in the estimated dielectric is relatively small, because the molarity is rounded and the error is only in non-significant figures. Compared to the error for the open coaxial transmission line, which had a maximum error of 1.3% for saline solutions [8], the solution presented in this thesis is comparable, but provided at a lower cost.

This empirical method is not without its faults. The method demonstrated here relies heavily on a base set of calibrations, and this set must be large enough to accurately characterize the material. For applications regarding surrogate brain gels (which was the original application), a characterization of samples of brain gels in various stages of degradation must be used for calibration. For these surrogate brain gels, the dielectric must be calculated using a different method, but the method presented in this thesis allows an empirical method to measure changes in the dielectric.

CHAPTER 6

SUMMARY, CONCLUSION, AND ACKNOWLEDGEMENTS

In this thesis, the goal was to measure the permittivity of various materials using shielded loop antennas and applied radio frequency (RF) energy. Originally structures of the shielded loop antenna and the experimental apparatus were modelled and simulated. The initial measurements were intended to compare the simulation results and the physical measurements. Because the simulation results did not line up, the simulations were not continued, but empirical measurements were continued.

By using a single shielded loop antenna, the input impedance of various saline solutions across frequencies from 0.1 to 2GHz were found. Using the peak input impedance from this frequency sweep, a valid empirical trend for the molarity of the solutions was found. Using this trend, various unknown molarities were tested and valid estimates were found. These estimates used a formula to accurately find the relative dielectric of a material. While this method is fairly accurate, this method requires a known method for finding the dielectric of the material studied, as well as a large enough set of measurements to accurately calibrate the relative changes in the dielectric material.

This project would not have been possible without the help and guidance of Dr. Aberle. The shielded loop antenna was provided courtesy of Dr. Diaz. In addition, Dr. Balanis allowed the use of his anechoic chamber for more accurate results, and Craig Birtcher, who assisted in taking measurements in the chamber. Dr. LaBelle and his PhD student, Chi Lin, also assisted by allowing a lab space and materials to mix saline solutions for testing.

REFERENCES

[1] Isaac Waldron, Thesis, Worchester Polytechnic Institute, Worchester, MA, 2006

[2] T. W. Athey, M. A. Stuchly and S. S. Stuchly, "Measurement of Radio Frequency Permittivity of Biological Tissues with an Open-Ended Coaxial Line: Part I," in IEEE Transactions on Microwave Theory and Techniques, vol. 30, no. 1, pp. 82-86, Jan. 1982.

[3] M. Kanda, "Standard probes for electromagnetic field measurements," in IEEE Transactions on Antennas and Propagation, vol. 41, no. 10, pp. 1349-1364, Oct 1993.

[4] C.A. Balanis, *Antenna Theory, Analysis, and Deisgn.*, 3rd edition, New York: Wiley, 1982, pp 231-275

[5] Timothy Bolton, Thesis, Georgia Institute of Technology, Atlanta, GA, 2016

[6] E. C. Burdette, F. L. Cain and J. Seals, "In Vivo Probe Measurement Technique for Determining Dielectric Properties at VHF through Microwave Frequencies," in IEEE Transactions on Microwave Theory and Techniques, vol. 28, no. 4, pp. 414-427, Apr 1980.

[7] N. Gavish, K. Promislow, *Dependence of the dielectric constant of electrolyte solutions on ionic concentration*, 2012.

[8] M. A. Stuchly, T. W. Athey, G. M. Samaras and G. E. Taylor, "Measurement of Radio Frequency Permittivity of Biological Tissues with an Open-Ended Coaxial Line: Part II - Experimental Results," in IEEE Transactions on Microwave Theory and Techniques, vol. 30, no. 1, pp. 87-92, Jan. 1982.